Insights into the role of lipoteichoic acids and MprF function in *Bacillus subtilis*

Aurélie Guyet[1]*, Amirah Alofi[1], Richard A. Daniel[1]*

[1] Centre for Bacterial Cell Biology, Baddiley-Clark Building, Biosciences Institute, Faculty of Medical Sciences, Newcastle University, Richardson Road, Newcastle upon Tyne NE2 4AX, United Kingdom.

*For correspondence Email: aurelie.guyet@newcastle.ac.uk and richard.daniel@newcastle.ac.uk Tel. +44 1912 083239.

Running title: Insights into the role of LTA in *B. subtilis*

Abstract

Gram-positive bacterial cells are protected from the environment by a cell envelope which comprises of layers of peptidoglycan that maintain the cell shape and teichoic acids polymers whose biological function remains unclear. In *Bacillus subtilis*, loss of all Class A Penicillin-Binding Proteins (aPBPs) which function in peptidoglycan synthesis is conditionally lethal. Here we show that this lethality is associated with an alteration of the lipoteichoic acids (LTA) and the accumulation of the major autolysin LytE in the cell wall. Our analysis provides further evidence that the length and abundance of LTA acts to regulate the cellular level and activity of autolytic enzymes, specifically LytE. Importantly, we identify a novel function for the aminoacyl-phosphatidylglycerol synthase MprF in the modulation of LTA biosynthesis in *B. subtilis* and *Staphylococcus aureus*. This finding has implications for our understanding of antimicrobial resistance (particularly daptomycin) in clinically relevant bacteria and the involvement of MprF in the virulence of pathogens, such as methicillin resistant *S. aureus*.

Keywords: *Bacillus*/ LTA/ LytE/ MprF/ PBP1

13 ## Introduction

14 Gram-positive bacteria have a common cell envelope architecture that contributes to maintaining
15 cell shape and protects the cell from environmental changes. The best characterised component
16 of the cell envelope is the peptidoglycan (PG) which forms a mesh like structure enclosing the
17 cell membrane. Onto this structure anionic polymers are either covalently attached to PG N-
18 acetylmuramic acids and known as wall-teichoic acids (WTA, **Fig 1A**) or are tethered to the
19 external face of the membrane and named lipoteichoic acids (LTA) (1-4). It is unclear whether
20 LTA are localized in a periplasm-like space between the membrane and PG or extend through
21 the PG layers (5, 6).

22 Peptidoglycan is synthetised by glycosyltransferases (GTases) which catalyse the addition of a
23 disaccharide pentapeptide precursor (lipid II), to the nascent PG chain (**Fig 1A**) while
24 transpeptidase (TPase) enzymes cross-link a proportion of the pentapeptides to adjacent PG
25 strands (7, 8). In the absence of the bifunctional transmembrane GTase and TPase enzymes,
26 known as class A Penicillin-Binding Proteins (aPBPs) (**Fig 1A**), *B. subtilis* cells are viable but
27 the cells are longer and thinner and are prone to lysis (9, 10). The viability of *B. subtilis* lacking
28 all aPBPs (referred as *Δ4*) depends on the functionality of the essential protein RodA that was
29 recently identified to function as a PG glycosyltransferase (11, 12). The *Δ4* strain is conditionally
30 lethal on PAB agar medium unless supplemented with magnesium (10). It is thought that this
31 divalent cation alters the structure of the wall by binding to teichoic acids or PG and by doing so,
32 might alter the activity of cell wall hydrolases (**Fig 1A**), the enzymes that modify and sculpt
33 synthesised PG to allow the cell to elongate and divide (5, 13-15).

34 In rod-shaped *B. subtilis* 168, LTA and WTA are composed of polyglycerolphosphate
35 (polyGroP) generated by independent biosynthetic pathways (**Fig 1B**) (2-5). Importantly, *B.*

36 *subtilis* is not able to survive the loss of both LTA and WTA synthesis (16) and these teichoic
37 acids seem to have roles in both cell growth (17) and division-separation (16, 18). It has also
38 been determined that anionic charge of these polymers can be modified by the addition of D-
39 alanine or N-acetylglucosamine (19). D-alanylation by Dlt proteins (**Fig 1A**) is proposed to
40 regulate autolysin activity, cell wall ion homeostasis (3, 5) and also imparts some resistance to
41 positively charged cationic antimicrobial peptides (CAMPs) (20). The net cell envelope charge is
42 proposed to be moderated by the teichoic acids and also the phospholipid composition of the cell
43 membrane (**Fig 1**) (21, 22). In this respect, the transmembrane protein MprF is the only enzyme
44 known to synthesise and translocate aminoacyl-phosphatidylglycerol (aaPGol), in particular
45 lysyl-PGol (**Fig 1**) (23-26). MprF plays a role in the virulence of bacterial pathogens (26, 27) and
46 in *B. subtilis,* it confers resistance to CAMPs (**Fig 1A**) such as nisin and daptomycin through
47 mechanisms that are not yet characterized (28, 29). Phosphatidylglycerol (PGol) is also the
48 substrate for LTA-synthases, in *B. subtilis* three of these enzymes are present: LtaS ('house-
49 keeping'), YfnI ('stress') and YqgS ('sporulation') (16, 18) (**Fig 1**). These transmembrane LTA-
50 synthases have an extracellular catalytic domain that uses PGol to generate a polyGroP polymer
51 on a lipid anchor (2, 3). The lipid anchor is usually a diglucosyldiacylglycerol (Glc_2DAG)
52 produced by UgtP on the internal surface of the cell membrane (30) (**Fig 1A**). As an *ugtP* mutant
53 still produces LTA (31), it suggests that polyGroP polymers are probably anchored to a
54 phosphatidylglycerol as observed in *Staphylococcus aureus* (32, 33).
55 In *S. aureus,* LTA is essential and seems to modulate autolytic activity (34), while WTA is
56 dispensable but appears to restrict autolytic activity (1, 4). Contrary to *B. subtilis*, *S. aureus* has
57 only one LTA-synthase (LtaS) whose absence is (conditionally) essential (35) and can be
58 complemented by *B. subtilis ltaS* but not *yfnI* (18, 36). A recent *in vitro* study showed that *S.*

59 *aureus* LtaS is processive and that the LTA polymer elongation is directly regulated by the
60 identity and concentration of lipid starter units. Interestingly, use of Glc_2DAG as a starter unit
61 led to the formation of shorter polymers (33) while the use of PGol resulted in the synthesis of
62 longer polymers. It is not clear if this newly identified mechanism might be conserved in *B.*
63 *subtilis.* However, in absence of *B. subtilis* LtaS, YfnI activity results in LTA of increased length
64 and it is possible that the combination of LtaS and YfnI activities modulated the length of LTA
65 (**Fig 1A**) (18, 37).
66 Through characterising *B. subtilis* strains lacking peptidoglycan GTase activity (12), we aimed
67 to understand the cell wall stresses causing aPBP mutants to lyse on glucose rich media.
68 Collectively, our data supports the idea that in *B. subtilis* LTA length acts to moderate the
69 activity of at least one important autolysin, LytE (**Fig 1A**). The presence of glucose in a strain
70 lacking aPBPs increases the expression of LtaS and YfnI and these result in altered LTA
71 production. Crucially, we identify a new role for MprF in altering LTA polymerisation in *B.*
72 *subtilis* and *S. aureus*. Our results reveal that MprF acts to change the cell envelope in a more
73 dramatic way than simply increasing the positive charge on the cell membrane which has
74 implications for understanding the association of MprF with both virulence and antibiotic
75 resistance in Gram-positive bacteria.

76 ## Results

77 **MprF alters cell viability in absence of *ponA* or *mbl***

78 In *Bacillus subtilis*, the absence of all aPBPs (*Δ4* for *ΔponA ΔpbpD ΔpbpF ΔpbpG* mutant) is
79 conditionally lethal on glucose-rich PAB agar medium unless supplemented with magnesium
80 (10, 12, 38). The suppressive effect of divalent magnesium has been observed in other cell-wall
81 deficient mutants (10, 16, 38, 39) and it is not well understood. To identify the cell wall factors
82 able to suppress *Δ4* lethality, we applied a random transposition mutagenesis to a strain deleted
83 for the vegetative aPBPs (**Tables 1-3**). Mapping of the transposon in strain SWA11a revealed an
84 insertion in the gene *mprF*, encoding a lysyl-phosphatidylglycerol (LysPGol) synthase known to
85 participate in phospholipid metabolism (**Fig 1**) (23, 28). Introduction of a *mprF* deletion into *Δ4*,
86 confirmed that *Δ4 ΔmprF* was viable on nutrient agar (NA) with glucose and on PAB agar (**Fig**
87 **2A, Fig S1A**). A strain lacking *ponA* (encoding the major aPBP (PBP1) is viable but exhibits a
88 growth phenotype that is suppressed by magnesium (**Fig 2A, Fig S1B**). Here the deletion of
89 *mprF* in *ΔponA* improved its growth and its colony morphology.

90 In the light of these results we reasoned that if MprF activity is detrimental to *Δ4* its
91 overexpression should be deleterious to *ΔponA*. Consistent with this, the overexpression of MprF
92 (MprF ↑) was found to be lethal in *ponA*-deleted strains on NA-glucose (**Fig 2B**). In contrast, on
93 NA, both *ΔponA* and *Δ4* strains grew slowly when *mprF* overexpression was induced (**Fig 2B**)
94 but no obvious effect was observed for 168CA or *Δ3* aPBPs (*ΔpbpD ΔpbpF ΔpbpG*). We also
95 observed that the overexpression of *mprF* caused the cells of *ΔponA* and *Δ4* to lyse in nutrient
96 broth (NB) (**Fig S1C**).

97 The identification of *ΔmprF* as a suppressor suggested that increased negative charge on the
98 membrane could contribute to the rescue of *Δ4* growth. This seemed to contradict the long-

99 standing hypothetical role of magnesium in altering the cell envelope by neutralizing anionic
100 polymers and/or autolysis activity (1, 5). As it is known that the function of *dlt* operon is to add
101 positive charge to LTA, it would be predicted that the loss of Dlt's function should have a similar
102 effect as *ΔmprF* on *Δ4* strain viability (40, 41). However, *Δ4 ΔdltAB* strain was unable to grow
103 on glucose rich media (data not shown). We also deleted the genes encoding the cardiolipin
104 synthases in *Δ4* to alter the membrane charge and the cellular pool of PGol (**Fig 1B**) but the loss
105 of cardiolipin had no suppressive effect on the *Δ4* phenotype (data not shown).
106 To understand if the effect of MprF was specific to *Δ4*, we altered MprF expression in other
107 known magnesium dependent mutants *ΔmreB* and *Δmbl*. It should however be noted that only
108 *Δmbl* requires magnesium to grow on plate compared to *ΔmreB* (**Fig S2A**). MreB, Mbl and
109 MreBH are actin-like isologues which help maintain cell shape by controlling both cell wall
110 synthesis (42) and the major autolytic enzymes CwlO and LytE (Mbl for CwlO and MreB/BH
111 for LytE) (43). Interestingly, we identified that MprF overexpression rescued the growth of *Δmbl*
112 on NA-glucose and NA (**Fig 2B**). In addition, the morphological defects associated with this
113 mutation (16) were less pronounced, resulting in wide rod-like shape cells and cell chains that
114 were less often twisted (**Fig 2C**).
115 To explain our genetic findings in *Δmbl* background, we had to consider that MprF might play a
116 role in cell wall metabolism. This idea seemed to be supported by transmission electron
117 microscopy (TEM) of a strain overexpressing MprF (**Fig 2FG**). Here cells exhibited an increase
118 in cell wall thickness (it was also observed that cell poles were 'dented', and septa were
119 misplaced), a defect similar to that observed in cell division mutants. However the change in cell
120 morphology of the strain deleted for *mprF* was less significant (**Fig 2E**).

121 Previous reports showed that lethality of *B. subtilis* Δ*mbl* is suppressed by the deletion of the
122 major LTA-synthase LtaS (16) and other work had shown that in *ltaS* mutant the activity of the
123 LTA-synthase YfnI results in longer LTA polymers (18). This suggested that the overexpression
124 of MprF in Δ*mbl* might diminish the cellular level of PGol (through a different pathway, **Fig 1B**)
125 (24) or MprF might function in LTA synthesis.

126 **Conditional essentiality of UgtP in the absence of MprF and the Class A PBPs**

127 To comprehend the effect of MprF-loss in a strain lacking aPBPs and identify the MprF
128 suppression pathway, we carried out a transposon screen in a strain lacking the vegetative class
129 A PBPs, *mprF, lacA* and carrying pLOSS-P_{spac}-*ponA* (strain AG200, **Tables 1-2**) (12) with the
130 objective of identifying alleles that rendered the maintenance of the plasmid copy of *ponA*
131 essential. From this screen strain AG200BK#42 was isolated with the expected phenotype and
132 found to carry a transposon inserted in the gene *gtaB*. GtaB catalyses a cytoplasmic conversion
133 of Glucose-1-P to UDP-Glc (**Fig 1**), where the latter ultimately contributes to LTA synthesis and
134 WTA modification. Subsequent mutagenesis in backgrounds *Δ4* and *Δ4 ΔmprF* confirmed the
135 lethal (NA-glucose) and sick (NA) phenotypes in absence of GtaB (**Fig 3A**).
136 To determine if this was related to LTA synthesis or WTA modification, we deleted sequentially,
137 in the *Δ4* or *Δ4* pLOSS-P_{spac}-*ponA* backgrounds, each enzyme whose function is immediately
138 upstream or downstream of GtaB (**Fig 1B)**. Characterisation of the resulting strains (**Table 2**)
139 showed that only deletion of *ugtP*, the enzyme which produces the Glc_2DAG lipid anchor for
140 LTA, had a similar effect to that of *gtaB*. Strain *Δ4 ΔmprF ΔugtP* was unable to grow on NA
141 glucose (**Fig 3A**), a phenotype common to *ΔponA ΔgtaB* and *ΔponA ΔugtP* (**Fig S2C**). On NA,
142 *Δ4 ΔgtaB* and *Δ4 ΔugtP* grew very slowly (**Fig 3A,** right panel).

143 LysPGol content increases in *ΔugtP* cells (24) which could explain the similarity of phenotype of
144 *Δ4 ΔugtP* and *Δ4* MprF ↑ (i.e. slow growing on NA) but not the dominant effect of *ΔugtP* on *Δ4*
145 *ΔmprF.* In *S. aureus,* it has been observed that *ΔugtP* (*ypfP*) and *ΔgtaB* mutants produce long
146 LTA (32). Thus this context and our results reinforced the idea that MprF may have a role in
147 LTA synthesis.

148 **Growth of a strain lacking all aPBPs mutant improves in absence of LtaS**

149 To verify that LTA synthesis alters *Δ4* growth, we analysed the phenotype of strains lacking
150 aPBPs and the LTA-synthase genes individually or in combination (**Fig 1**). Surprisingly, the *Δ4*
151 *ΔltaS* mutant was viable on NA-glucose as well as with the additional deletion of *yfnI* or *yqgS*
152 (**Fig 3B**). Other strains expressing LtaS showed limited growth and were found to pick up
153 suppressor mutations rapidly on glucose (e.g. *Δ4 ΔyfnI*, *Δ4 ΔyfnI ΔyqgS,* **Fig 3B**). Thus, LtaS
154 activity is also linked to the glucose-associated lethality of *Δ4.* Interestingly, the absence of
155 MprF is more advantageous to *Δ4,* as it results in a faster growth and larger colonies formed on
156 NA-glucose compared to *Δ4 ΔltaS* (**Fig S1B**). This phenotypic difference indicated that slightly
157 different mechanisms helped restore the growth of *Δ4*.
158 To test this, LTA-synthase genes were systematically deleted in the *Δ4 ΔmprF* (AG223)
159 background and the viability of the strains generated determined on NA with or without glucose.
160 All the strains remained viable on NA glucose (**Fig 3C**) which indicated the effect of MprF loss
161 could be related to LTA. In support of this, in the *Δ4 ΔmprF* background the combined absence
162 of *ltaS* and *yfnI* delayed growth on NA glucose resulting in a phenotype similar to that observed
163 on NA (**Fig 3C)**. Thus, in these specific genetic backgrounds LTA synthesis is not essential but
164 permitted higher growth efficiency.

165 Neither the absence of LtaS nor MprF had any effect on the filamentous thin cell morphology of
166 *Δ4* (**Fig S3A-B, Table 4**) but cell lysis was significantly decreased in NB. In the absence of all
167 LTA-synthases, *Bacillus* is viable but the strain forms filamentous and clumpy cells (16). We
168 observed that the combined absence of LtaS, YfnI and/or YqgS in *Δ4, ΔponA* or *Δ4 ΔmprF*
169 genetic backgrounds lead to an increase in cell diameter and cells remained linked together at the
170 site of division (**Fig 3D, Fig S3A-B, Table 4**). However, when LtaS was the only functional
171 LTA-synthase (e.g. *Δ4 ΔyqgS ΔyfnI*, **Fig 3D**), cells were thin and comparable to *Δ4* and the
172 *ΔponA* background (**Fig S3C-D**). Collectively, our results indicate that the activity of the LTA
173 synthases, in particular LtaS activity, could account for *Δ4* phenotype.

174 **Impact of glucose, PBP1 and MprF on LTA synthesis.**

175 To comprehend the effect of LtaS, MprF and UgtP in the absence of aPBPs we decided to
176 analyse LTA production. We developed a Western blot protocol relying on a monoclonal
177 antibody for Gram-positive LTA (Thermofischer) and a polyclonal PBP2B antibody. First, we
178 determined the LTA profile for 168CA and the LTA-synthases mutants (**Fig 4A** and **Fig S4**)
179 grown in NB and NB glucose (0.2%). The wild type LTA signal corresponded to a mobility
180 comparable to 7-17 kDa as previously identified (18). Interestingly, our media comparison
181 showed that LTA-signal in *ΔltaS* cells grown in NB-glucose (> 15 kDa) (**Fig 4A** left panel, 2nd
182 lane) was distinct from that seen for growth in NB (7-32 kDa) (**Fig 4A** right panel, 2nd lane).
183 However, the LTA pattern was different when YfnI was the only functional LTA-synthase (**Fig**
184 **4A**). From this analysis, short LTA (<10 kDa) were more abundantly produced in NB-glucose.
185 This seemed to be related to LtaS activity, as we observed an increase in short LTA in *ΔyfnI* and
186 *ΔyfnI ΔyqgS* mutants compared to 168CA (**Fig 4A** left panel, 3rd & 5th lanes). Collectively, our

187 results show that the regulation of LTA synthesis is more complex than thought (18) as it
188 influenced by the metabolic/nutritional status of the cells.
189 As the *mprF* mutation suppressed the *ΔponA* phenotype (**Fig 2A, Fig S1B**) we reasoned that any
190 alteration of LTA synthesis would be detectable in a strain where only the major aPBP was
191 deleted. As the multiple aPBP deletion strain was very lytic and did not grow under certain
192 conditions (**Fig S1**), further experiments were done in the *ΔponA* background. Using this
193 background, strains could grow in NB glucose 0.2% and this permitted the preparation of
194 samples for the Western blot analysis. Analysis of *ΔponA* cells grown in the presence of glucose
195 revealed that there was an increase in short LTA that was not evident in the absence of glucose
196 (**Fig 4B** left panel, 3rd lane, **Fig S5D**). In comparison, the LTA signal of *ΔponA ΔmprF*
197 decreased compared to *ΔponA* (**Fig 4B** left panel, 5th lane) and the *ΔmprF* mutant in NB-glucose
198 (**Fig 4B** left panel, 4th lane) decreased compared to that of 168CA (**Fig S5D**). Surprisingly, we
199 found that *mprF* overexpression (MprF ↑) had a significant effect, resulting in an increased LTA
200 polymer length (6th lane in **Fig 4B)**. This effect was independent of YfnI, as a similar LTA
201 profile was observed in a strain *ΔyfnI* MprF ↑ while the profile of a *ΔltaS* MprF ↑ was similar to
202 that of *ΔltaS* (data not shown, strains AG353 & AG349 in **Table 2**). The latter was expected as
203 LtaS activity seems dominant over YfnI (18). The overexpression of *mprF* in *ΔponA* cells
204 resulted in a broader size range of LTA than that seen for the wild type as we observed an
205 increase in LTA signals below 10 kDa but also above 15 kDa (7th lane in **Fig 4B, Fig S5D**). This
206 to some extent resembled that observed in single mutants *ΔponA* and MprF ↑, respectively. Thus,
207 the cumulative effect of the mutations had led to an increase in LTA length range and could
208 explain the lethality of the *ΔponA* MprF ↑ double mutant on NA-glucose-IPTG (**Fig 2B**).

209 Western blot analysis of the LTA in the *Δmbl* background showed that it was weak, and
210 representative of short LTA (second to last lane **Fig 4B, Fig S5D**). Overexpression of *mprF*
211 rescued *Δmbl* growth (**Fig 2B**) and this overexpression resulted in an increased in LTA length
212 and abundance in the *mbl* background (last lane **Fig 4B**). This result was also consistent with
213 what was observed for *Δmbl ΔltaS* with the detection of longer LTA polymers (data not shown)
214 similar to that of *ΔltaS* (**Fig 4A**). Thus an increase in LTA length seems to characterize the effect
215 of these two *Δmbl* suppressor mutations.
216 Analysis of the suppressor *ΔltaS ΔponA* revealed the dominance of *ltaS* deletion, in that the LTA
217 exhibited a retarded migration (3rd lanes in **Fig 4C, Fig S6**), similar to that observed in *ΔltaS*
218 (**Fig 4C**). In absence of UgtP which produces a lipid anchor Glc_2DAG (**Fig 1**), we observed an
219 increase in LTA length in both media conditions, but the shift was more distinct in glucose (>12
220 kDa, left panel 4th lane in **Fig 4C**). The latter is comparable to the LTA signal detected in the *S.*
221 *aureus ΔugtP* mutant grown in TSB, a glucose rich medium (32). Analysis of *ΔponA ΔugtP,*
222 which was conditionally lethal on NA-glucose (**Fig S2C**), revealed an increase of the LTA-
223 signals and length (7-25 kDa, left panel 5th lane, **Fig 4C**), a pattern reminiscent of that
224 determined for *ΔponA* MprF↑ strain (left panel 7th lane in **Fig 4B)**, which was also lethal on NA-
225 glucose (**Fig 2B**).
226 To conclude we show the first evidence that MprF activity has a role in altering the length of
227 LTA, through a LtaS-dependent mechanism and has an impact on cell wall metabolism. Our
228 results also highlight that the conditions leading to the lethality of *ponA* are associated with an
229 increase in the abundance and length of LTA.

230 **Overexpression of major autolysin LytE is lethal in absence of PBP1 or LtaS**

231 Our results inferred that the conditional lethality of aPBPs mutant might be linked to an interplay
232 between LTA length and autolysin activity. Autolysins or cell wall hydrolases help shape and
233 recycle the peptidoglycan during cell elongation and division. *B. subtilis* expresses a large
234 number of them but only the loss of both PG D,L-endopeptidases CwlO and LytE is lethal (13,
235 14, 44-46) (**Fig 1A**). We focused on LytE because it is considered to be one of the key
236 autolysins, it is secreted and thought to be anchored to the lateral cell wall and the septum in a
237 way that is influenced by the teichoic acids (43). LytE abundance also increased in *ΔltaS* (47)
238 and both LtaS and LytE affect colony development (48) and cell diameter (16, 43).

239 We reasoned that if an imbalance of LytE activity existed in the aPBPs mutants (*Δ4* and *ΔponA*)
240 grown in glucose-rich medium, then a deliberate increase in LytE expression should exacerbate
241 the strain phenotype, leading to cell death. Interestingly, *lytE* overexpression (by IPTG induction
242 of a $P_{hyspank}$-*lytE* allele) was found to be lethal in both *Δ4* and *ΔponA* backgrounds when grown
243 on NA-glucose and it significantly delayed the growth of *Δ4* and *ΔponA* on NA but not that of *Δ3*
244 *ponA+* (**Fig 5A, Fig S7A**). This result confirmed that an imbalance in autolytic activity was
245 detrimental to the cell that had lost PBP1. Importantly, the overexpression of *lytE* in the *Δ4*
246 *ΔltaS, ΔponA ΔltaS* and *ΔltaS* strains was lethal (**Fig 5A**) while the growth of *ΔponA ΔmprF* was
247 only slightly delayed. However, the overexpression of *lytE* in *Δ4 ΔmprF* severely perturbed its
248 growth on glucose but the strain remained viable. In contrast, the control strain with only the
249 *ΔmprF* mutation was unaffected by *lytE* overexpression.

250 This finding suggested that *ΔponA ΔltaS* and *ΔponA ΔmprF* mutants, which have distinct LTA
251 length, were differently sensitive to LytE activity. Therefore, we examined the double LTA-
252 synthase mutant backgrounds, here we found that only the strain expressing *ltaS* was viable

253 when *lytE* was overexpressed (**Fig 5A,** last strain). In these genetic backgrounds, the absence of
254 *mprF* or *ugtP* had no effect (data not shown). Interestingly, *ΔltaS* LytE ↑ was viable on NA (**Fig**
255 **5A,** 8th strain) but not on NA-glucose while we previously identified that *ΔltaS* produces distinct
256 LTA length on each of these media (**Fig 4A**). Thus, it is clear that the activity of LtaS, is required
257 for the cell to balance the effect of overexpression of *lytE*, presumably by producing a specific
258 LTA length.
259 To comprehend the apparent tolerance of $LtaS^+$ and *ΔmprF* cells to LytE, we constructed an
260 unstable replicon pLOSS-P_{spac}-*lytE* plasmid which expresses *lytE* at a level lower than $P_{hyspank}$-
261 *lytE* (**Table 1**). This plasmid in the *ΔmprF* strain was retained in all media conditions tested
262 (AG1481 strain), including elevated magnesium. This was indicated by the fact that the colonies
263 remained blue on IPTG XGal supplemented media (**Fig 5B**) whereas other strains tested showed
264 instability of the plasmid (e.g. 168CA, *ΔponA, ΔponA ΔmprF* and LTA-synthases mutants,
265 **Table 2**) an indication that there was no selective advantage for the cells to maintain the plasmid.
266 Thus this plasmid stability assay highlights that *ΔmprF* cells tolerate higher expression of *lytE*
267 compared to the other background strains tested. At this stage, it is unclear if the *ΔmprF* strain's
268 tolerance for *lytE* overexpression is due to the loss of aaPGols or the production of shorter LTA
269 or both.

270 **LTA influences LytE activity**

271 The conditional lethality observed when overexpressing *lytE* prompted us to investigate the
272 cellular levels of this autolytic enzyme in our strains. First, we engineered strains that could
273 express a recombinant protein LytE-$LEMGRSH_{12}$ (using pMUTin-*'lytE-his,* **Table 1**) and then
274 analysed total lysates by Western blot using anti-histidine (for LytE) (**Fig 5C, Fig S7B**) and an

275 anti-LtaS antibody raised against LtaS (74 kDa) that cross reacts with YfnI (73 kDa) (**Fig 5D,**
276 **Fig S8A**). This showed that LytE and LtaS/YfnI accumulate in *ΔponA* cells, particularly when
277 grown in presence of glucose (**Fig 5C-D**). Using a set of strains that had either pMUTin-*'ltaS-his*
278 or pMUTin-*'yfnI-his* integrated into the genome, we could confirm that both LtaS and YfnI are
279 more abundant in *ponA* cells (**Fig S8B, Tables 1-3**).
280 In *ΔponA ΔmprF*, LytE and LtaS/YfnI protein levels were lower compared to *ΔponA* (**Fig 5C-D**),
281 but no obvious change was observed in the wild-type background (WT*) and *ΔmprF* strains.
282 *ΔltaS* and *ΔponA ΔltaS* exhibited an increase in both LytE and YfnI when grown in NB-glucose,
283 an effect more pronounced in the *ΔponA ΔltaS* mutant (**Fig 5C-D**, left panel). In addition,
284 comparative analysis of the set of LTA-synthase mutants (**Fig S8C**) revealed that LtaS/YfnI
285 increased in presence of glucose and in the absence of YfnI, LtaS increased significantly. Also,
286 and potentially more importantly, in the absence of LtaS, LytE abundance increased. Analyses of
287 the strains that were lytic under the same growth conditions showed that there was an excess of
288 LtaS/YfnI in *ΔponA ΔugtP* and *ΔponA* MprF ↑ cells cultured in either NB or NB-glucose (**Fig**
289 **S9B-C,** e.g. 6-7th lanes). It was also evident that LytE was more abundant than the wild type.
290 These observations seem to support the idea that the altered abundance of these proteins,
291 identified in *ΔponA* cells, was associated with the sick phenotype.
292 Taken together, our results show a correlation between LTA length and LytE abundance in the
293 cell which suggests that LTA acts to moderate cell wall metabolism. In *ponA* mutants, this
294 function is unbalanced such that cell wall degradation is predominant. This is summarised in the
295 discussion in **Fig 7**.

296 **LTA production is altered in *S. aureus ΔmprF* and is an important factor in *B. subtilis***
297 **sensitivity to daptomycin**

298 MprF is conserved in the *Firmicutes* and has been shown to contribute to *S. aureus* pathogenicity
299 (21, 22). Importantly, studies of clinical isolates have found that methicillin-resistant *S. aureus*
300 strains (MRSA) that have acquired resistance to daptomycin (Dap^R), a lipopeptide antibiotic that
301 acts to interfere with membrane containing phosphatidylglycerol (26, 49-51), frequently carry
302 nucleotide polymorphisms (SNPs) in *mprF* (52, 53). Although some *mprF* SNPs were associated
303 with a MprF gain of activity (increasing LysPGol and reducing PGol), others had no clear
304 correlation between the phospholipids composition and the relative surface charge of the cell
305 (26). In this context, we asked whether the role of MprF in LTA production is conserved in *S.*
306 *aureus* as it seemed reasonable that this might contribute to Dap resistance. Analysis of LTA
307 production in methicillin sensitive *S. aureus* strains showed that the LTA from the *mprF* mutant
308 migrated faster than that of the wild type SA113 (**Fig 6A, Fig S10A**), thus LTA production is
309 altered in *S. aureus ΔmprF*. Interestingly, when exposing exponentially growing cells of *S.*
310 *aureus* to daptomycin, our analysis showed that the LTA length and production had increased in
311 both strains (**Fig. S10B-C**, samples treated with 0.25 and 0.5 µg/ml DAP for *ΔmprF* and the wild
312 type, respectively). It is also noteworthy that even when exposed to DAP, the LTA produced by
313 the wild type remained longer than that of the *ΔmprF* mutant, which perhaps indicates that the
314 LTA length plays a role in DAP sensitivity. This effect was observed at DAP concentrations that
315 did not significantly impacted on the wild type growth (**Fig. S10E**) whereas the growth of the
316 *mprF* mutant was significantly impaired (**Fig. S10D-E**), as previously reported (52, 53). Our
317 results seem to confirm that MprF's role in modulating LTA production is conserved in both
318 *Bacillus* and *Staphylococcus* species. Collectively, these results indicate that a change in LTA

319 nature and/or production, rather than an alteration in membrane properties, might be associated
320 with Dap resistance in *S. aureus*.
321 As we could not carry analysis on Dap^R MRSA (laboratory regulations), we, therefore, turned
322 our interest to the strongest known Dap^R allele in *B. subtilis, pgsA A64V* (54). This mutation of
323 the essential gene *pgsA,* encoding the PGol-synthase (**Fig 1B**), has been shown to reduce cellular
324 PGol content and was suggested to modify LTA production (54). Thus, we analysed the LTA of
325 *B. subtilis* wild type (WT), isogenic strains carrying *pgsA^{A64V}* (strains Dap^R 1 & Dap^R 20) and
326 *pgsA^{A64V}* complemented with *pgsA*^{WT} grown overnight in NB **(Fig 6B, Fig S10F)**. Our assays
327 revealed that no LTA signal was detected below 30 kDa in Dap^R strains whereas LTA was
328 detected in the strains complemented for *pgsA* (Dap^R *pgsA*^{WT}) that were similar to that of the
329 wild type strain. Thus, PgsA A64V accounts for the severe reduction in LTA production. Finally,
330 we verified that the two major LTA-synthases were still produced in Dap^R strains by Western
331 blot (**Fig 6B, Fig S10F**). A strong LtaS/YfnI signal was detected in Dap^R strains which proved
332 that one or both LTA-synthases were still expressed, but up-regulated.
333 The above findings in *S. aureus* and *B. subtilis* suggested that alteration in LTA could be
334 associated with DAP sensitivity. As *S. aureus ltaS* is essential, we decided to analyse the Dap-
335 sensitivity of *B. subtilis* expressing only one LTA-synthase. Our assays on NA (**Fig 6C**) and NB
336 (**Fig. S10G**) showed that strains lacking the major LTA-synthase LtaS were sensitive to DAP
337 and this sensitivity was higher than that observed for *ΔmprF* or *Δdlt* mutants (**Fig S10G**). Thus
338 LtaS activity is required for DAP tolerance in *B. subtilis*, more so than MprF.

339 ## Discussion

340 In absence of the class A PBPs (*Δ4*), *B. subtilis* is viable due to the presence of RodA, the
341 essential PG glycosyltransferase (controlled at least in part by the cell envelope stress regulator
342 σ^M (11, 12)) and yet lethal on glucose rich medium (**Fig 2A** & **S1B**). By studying either *Δ4* or
343 *ΔponA* single mutant, we now understand that the presence of glucose leads to an increase in
344 abundance of the LTA-synthases LtaS and YfnI. The increase in these enzymes results in altered
345 LTA production that in turn causes the accumulation of major autolysin LytE (**Fig 4-5**), the end
346 result being cell lysis through the inability to regulate the activity of autolysins (**Fig 7**). This lytic
347 phenotype could be suppressed by the absence of MprF (**Fig 2A, S1B**), an enzyme that we think
348 helps in the regulation of LTA production (**Fig 8**). In *ΔponA,* loss of MprF resulted in reduced
349 LTA production and decreased level of LytE (**Fig 4B, 5C, S5D**). This was consistent with our
350 finding that an increase in length and abundance of LTA (overexpression *mprF*, *ΔugtP*) and/or
351 an increase in LytE correlated with glucose-mediated lethality in *ΔponA* (**Fig 2B, 3A, 4B-C, 5A,**
352 **S5D, Fig S9B-C**). Loss of major LTA-synthase LtaS was not as beneficial for the growth of *Δ4*
353 as the loss of MprF (**Fig 3B, S1B**). In *ΔponA,* loss of LtaS lead to the production of very long
354 LTA polymers similar to the single *ltaS* mutant and a persisting high level of LytE (**Fig 4C, 5C**).
355 This might explain why the growth of *ΔponA ΔltaS* was not significantly enhanced compared to
356 *ΔponA* (**Fig S1B**). In support of this, the analysis of strains only defective in LTA synthesis (last
357 three rows in **Fig 5A**) indicated that LtaS presence is required to prevent cell lysis when *lytE* was
358 artificial overexpressed (**Fig 5A, 7**), presumably because a distinct LTA length (7-17kDa) and/or
359 abundance similar to the wild type LTA (**Fig 4A**) is required (**Fig 7**).
360 Previous studies have suggested that LTA could inhibit autolysins activity (1, 5) but the key
361 factors involved have not been identified. Recent work in *S. aureus* showed a *ΔugtP* mutant

362 producing long LTA is susceptible to PG hydrolases (55) and it has been suggested that major
363 autolysin LytA is sequestered by LTA in exponential growth (56). Our results indicate that LytE
364 in *B. subtilis* exhibits similar characteristics and that the length of LTA has a role in modulating
365 LytE abundance or presumably its activity (**Fig 7**). However it is unclear how this mechanism
366 may work in relation to the localisation of the LTA in the wall relative to active autolysins,
367 particularly LytE, and this remains an important question to answer in future work.
368 In *B. subtilis* 168, expression of *lytE* is quite complex and coordinated by regulators such as σ^I
369 and WalR (46, 57). In contrast, transcriptional regulation of *mprF* is not well defined, but
370 interestingly analysis of *B. subtilis* BSB1 showed that *mprF* and *pgsA* expression is positively
371 correlated with that of *walKR,* the two-component response system that controls cell wall
372 metabolism, and notably *lytE* (cluster A418 in Subtiwiki expression data browser; (58, 59)).
373 However, expression of *walKR* and *sigI* is not significantly altered in LB-glucose (58) or in the
374 absence of aPBPs (12) but theses regulators might play a post-transcriptional role in *Δ4* where
375 the σ^M cell wall stress response is active (12, 57). This seems to be supported by the fact that
376 some of the cell wall associated genes mentioned (*sigM*, *ponA*, *ltaS*, *yfnI*, *mprF*, *pgsA*) are
377 differently expressed in cells of *B. subtilis* BSB1 in LB-glucose (58, 59). Thus *B. subtilis* might
378 need to adapt its cell wall metabolism in response to glucose and this might account for the
379 partial redundancy of function of *B. subtilis* LTA-synthases. Evidence also suggest that the
380 presence of magnesium in culture medium leads *Bacillus* cells to adjust its cell wall metabolism.
381 When we looked at the effect of magnesium in presence of glucose on aPBP mutants, as this is
382 known to suppress the growth defect (10), we have observed that magnesium decreased the
383 abundance of LytE significantly in *ΔponA* and *ΔponA ΔmprF* (**Fig S9**) but not as much in *ΔponA*
384 *ΔltaS.* In addition, high levels of magnesium have an impact on LTA production (work in

385 progress) and other processes (60, 61). Thus, the mechanism by which exogenous magnesium
386 helps the growth of some cell wall mutants might partially require LtaS activity to tune LytE
387 abundance in the cell wall (14). Altogether, our study brings a new perspective on the
388 importance of LTA in the cell envelope stability and how the extracellular biosynthesis is
389 regulated.
390 In this study, we have identified a new function for MprF, an enzyme known to synthetise
391 aminoacyl-phosphatidylglycerol (aaPGol) phospholipids and translocate them across the
392 membrane (**Fig 1**). We show that MprF activity impacts the biosynthesis of LTA (**Fig 8A**) and
393 this in turn alters cell wall metabolism. The LTA profiles observed in *B. subtilis* and *S. aureus*
394 lacking MprF (seen as shorter and/or decreased in abundance) and the overexpression of *B.*
395 *subtilis* MprF (causing a smeared & retarded mobility of the LTA) (**Fig 4B, 6A**) suggest that
396 MprF positively regulates LTA production (**Fig 8A**). Other studies have indicated that MprFs
397 may have relaxed substrate specificities across species (22, 62) and even synthetise lysyl-
398 glucosyl-DAG glycolipid in *Streptococcus agalactiae* (63). Recently, it has been shown that
399 when *S. aureus* LtaS uses PGol as an alternative anchor to the glycolipid produced by UgtP, the
400 concentration of these free lipid starter units regulates the length of the LTA polymerised *in vitro*
401 (33). Thus it is possible that MprF activity contributes to LTA synthesis (**Fig 8B**). MprF might
402 provide the last capping unit (Lys-, Ala-GroP) to LtaS to terminate the LTA being polymerised,
403 this would also contribute to the protection against CAMPs (**Fig 8B**). Alternatively, aaPGols
404 might be a source of GroP units (**Fig 8B**) in the formation of LTA in addition to the known PGol
405 source altering processivity (33). Another possibility would be that aaPGols change the
406 electrostatic environment and this impacts on LTA-synthase(s) activity by keeping the LTA
407 polymers adjacent to the membrane (**Fig 8B**).

408 Gain of function in MprF has been identified in methicillin-resistant *S. aureus* (MRSA) clinical
409 isolates that have acquired resistance to daptomycin (Dap), an antibiotic used as a last resort to
410 treat MRSA infections (26, 53). Over the years, MprF-mediated resistance to Dap (Dap^R) has
411 been investigated but a consensus model has yet to link Dap^R to a particular domain of MprF
412 and/or to a particular LysPGol content in one or both membrane leaflets (26, 64). In *B. subtilis,*
413 our analysis shows the significant decrease of LTA produced in a strain with the *pgsA A64V*
414 mutation (**Fig 6B**), a strain with a reduced PGol content that exhibits Dap resistance (54). Also,
415 we found that LTA-synthase LtaS is required for DAP tolerance in *B. subtilis* (**Fig 6C**). The
416 function of MprF in LTA synthesis and the new understanding of *S. aureus* LtaS processivity
417 (33) could be the link with the alleles *cls* encoding a cardiolipin synthase, *pgsA* and *dlt* operon
418 (50) identified in *S. aureus* MRSA that result in Dap resistance. Together, these findings support
419 the idea that a modification in LTA polymerisation in addition to D-alanylation of teichoic acid
420 (65, 66) could result in a cell envelope that is less permeable to Dap, and not necessarily linked
421 to increased cell wall thickness (67). Further analysis of LTA synthesis and cell wall
422 composition will help redefine MprF-mediated Dap^R mechanism and help appreciate the exact
423 role of MprF in the net cell surface charge and the protection against cationic antimicrobial
424 peptides. Recent research on compounds targeting LTA synthesis (68, 69) and on MprF-targeting
425 monoclonal antibodies (70) suggest these approaches have relevance in combating clinically
426 relevant bacteria.

427 ## Material and Methods

428 ***Plasmids, bacterial strains, and primers***

429 Plasmids and strains used in this study are listed in **Tables 1** and **2.** Strains constructions are
430 described below or in **Table 2** (last column). Primers used are listed in **Table 3.**

431 ***Growth conditions and general methods***.

432 *B. subtilis* strains were grown routinely on nutrient agar (NA, Oxoid) or in nutrient broth (NB,
433 Oxoid). For some assays, strains were grown in liquid Difco antibiotic medium 3 (PAB, Oxoid)
434 and PAB agar (15 g/l agar, Oxoid). *B. subtilis* transformations were carried out as previously
435 described using SMM defined minimal medium (71, 72). *B. subtilis* was usually incubated at
436 30°C (overnight), next day cells were diluted and grown at 37°C (unless specified differently).
437 *Escherichia coli* and *Staphylococcus aureus* strains were incubated at 37°C on NA plate or in
438 Luria-Bertani (LB). PCR, plasmid manipulations, and *E. coli* transformation were carried out
439 using standard methods. Strains were selected on NA supplemented with ampicillin (for *E. coli,*
440 200 µg/ml), spectinomycin (60 µg/ml), kanamycin (5 µg/ml), phleomycin (1 µg/ml),
441 erythromycin (0.5 µg/ml), chloramphenicol (5 µg/ml) and daptomycin (see later). Various
442 supplements were also used: IPTG (isopropyl-β-D-thiogalactopyranoside, 0.1 or 1 mM), X-Gal
443 (5-bromo-4-chloro-3-indolyl-β-D-galactopyranoside, 100 µg/ml), $MgS0_4$ (between 5 mM to 25
444 mM as required), and glucose (final concentrations up to 1%). For NA plates supplemented with
445 20 mM $MgSO_4$, the concentration of spectinomycin, kanamycin and erythromycin antibiotics
446 was doubled to avoid growth of false positive strains. Strains with the pMUTin-*his* integration
447 were always grown in presence of erythromycin.

448 ***Plasmids constructions***

449 To obtain pDR111-$P_{hyspank}$-*mprF* plasmid, the *mprF* (BSU_08425) coding sequence was
450 amplified using primers oAG271-272, which changed the start codon (from TTG to ATG). The
451 PCR product and pDR111 plasmid (**Table 1**) were digested by *Sal*I and *Sph*I restriction
452 enzymes, ligated together and transformed into *E. coli* DH5α. Digestion and PCR sequencing
453 using primers oAG300-301 verified the presence of the insert.

454 To construct pDR111-$P_{hyspank}$-*ltaS*, pDR111-$P_{hyspank}$-*yfnI* and pDR111-$P_{hyspank}$-*yqgS,* each LTA-
455 synthase gene was amplified by PCR with primers pairs oAG308-309 (2064 bp), oAG310-311
456 (2078 bp) and oAG312-313 (1990 bp), respectively. PCR products were digested by *Nhe*I and
457 *Sph*I, each ligated with the plasmid pDR111 digested with the same restriction enzymes. The
458 next steps were carried out as described for pDR111-$P_{hyspank}$-*mprF*.

459 For pLOSS-P_{spac}-*lytE, lytE* was amplified by PCR with oAG348-349 (1143 bp) primers*,* and the
460 PCR product inserted in pLOSS* (**Table 1**) as a *Not*I and *Bam*HI fragment. After transformation,
461 the resulting plasmid was checked by PCRs with primers oAG18-19 and finally checked by
462 sequencing.

463 To construct the plasmids pMUTin-*'lytE-his*, pMUTin-*'ltaS-his* and pMUTin-*'yfnI-his* the 3'-
464 terminus part of gene of interest gene (except for the stop codon) was amplified with primer pairs
465 oAG354-355, oAG366-367 and oAG360-361, respectively to obtain a PCR products ranging
466 from 288 to 309 bp. The PCR products and the plasmid pMUTinHis (**Table 1**) (73) were
467 digested by *Eco*RI and *Xho*I, ligated together and transformed into *E. coli* DH5α. Each insertion
468 '*lytE, 'ltaS* and *'yfnI* was verified by PCR and plasmid sequencing using primers oAG368-369.

469 To construct pAM-21, plasmid pET28a (+) (Novagen) and *lytE* (from the 76th bp, removing the
470 coding sequence for the signal peptide) were amplified by PCRs using primer pairs oAA01-02

471 and oAA03-04, respectively. DNA fragments generated were assembled using NEBuilder HiFi
472 DNA assembly kit (NEB). The resulting plasmid was verified by sequencing using primers
473 oAA05-06.

474 ***Bacillus directed mutagenesis***

475 Steps leading to construction of new mutants are indicated in the last column of **Table 2** with
476 additional details in this section. New mutants were often obtained by transformation of
477 competent cells with a clean genomic DNA extracted from another existing *B. subtilis* mutants.
478 Construction of some of the markerless class A PBPs mutants were previously described (12).
479 Additional mutants described in this study were obtained using the plasmids pG+host9::*ΔponA,*
480 pG+host10::*ΔpbpD,* pG+host10::*ΔpbpF* (**Table 1**) (12). PCR with primers oAG124 to oAG129
481 were consistently performed to check markerless deletions were not lost (12).
482 All transformations of the background strain with, and/or leading to, deletion of *ponA, mreB,*
483 *mbl, gtaB, ugtP, ltaS* were selected for on NA medium supplemented with $MgSO_4$ (20-25 mM)
484 with the appropriate antibiotic.
485 To construct strain AG181 (*ΔmprF*), DNA fragments upstream and downstream the *mprF* coding
486 sequence were amplified by PCR using primers oAG103-104 (2390 bp) and oAG105-106 (2414
487 bp), respectively and were digested by *Eco*RI and *Xba*I, respectively. The phleomycin resistance
488 antibiotic cassette was amplified by PCR with primers PhleoXbaIfor and PhleoEcoRIrev from
489 plasmid pIC22 and digested by both *Eco*RI and *Xba*I. The 3 digested PCR-fragments were
490 ligated to generate a linear DNA, transformed into 168CA with selection for phleomycin
491 resistance. The deletion of *mprF* was confirmed by PCR using primers oAG107-108.

492 Strain AG304 (*amyE::*$P_{hyspank}$*mprF, spc*) was obtained by transformation of 168CA with
493 pDR111-$P_{hyspank}$-*mprF* plasmid (**Table 1**). Correct recombination was confirmed by the absence
494 of amylase activity when grown on NA with 0.2% starch and by PCR (oAG300-301 primers).
495 The same methods were used after transformation of other pDR111-derivatives.
496 We constructed our own *lytE* deletion mutant (Δ*lytE::cat*). For this, regions of genomic DNA
497 upstream and downstream of *lytE* were amplified by PCRs with oAG350-351 (2048 bp) and
498 oAG352-353 (2500 bp) primers pairs, respectively. These products were then digested by *Xba*I
499 or *Bam*HI (**Table 3**). The chloramphenicol resistance cassette from pCotC-GFP plasmid (**Table**
500 **1**) was amplified with primers oAG197-198. The resulting PCR products (850 bp) was then
501 digested by *Xba*I and *Bam*HI and the three DNA fragments were ligated and transformed into *B.*
502 *subtilis* 168CA. Strain AG547 was obtained from this transformation and the deletion of *lytE*
503 confirmed by PCR using primers oAG340-341 (**Table 3**).
504 Strains AG565 and AG586 were obtained by integration of pMUTin-'*lytE-his* (erythromycin
505 selection) in 168CA and Δ*cwlO* (AG474 strain) background, respectively. The plasmid
506 integration (single cross-over) in *B. subtilis* resulted in expression of recombinant proteins with
507 LEMRGSH$_{12}$ tag in C-terminus, under the control of its native promoter. Since the integration of
508 this plasmid into the Δ*cwlO* background did not result in any phenotypic change it indicated that
509 the LytE-His$_{12}$ was functional, as a double mutant *lytE cwlO* is lethal (44). Thereafter, genomic
510 DNA of AG565 strain was used to transform all the strains needed for Western blot analysis
511 (**Table 2**). Of note, AG1541 strain (Δ*cwlO*) obtained by genomic DNA recombination has the
512 same genotype as AG586 strain obtained by plasmid integration.

513 ***Random transposition mutageneses***

514 Random transposition mutageneses were performed as previously described (39, 74) using the
515 pMarB plasmid that carries the transposon TnYLB-1 encoding kanamycin resistance. pMarB
516 was introduced into *B. subtilis* strains carrying pLOSS-P_{spac}-*ponA* (12) (**Table 1**), a plasmid with
517 an unstable origin of replication and *lacZ* which helps to monitor the plasmid stability by
518 observing formation of blue or white colonies. After screening the random library of mutants,
519 genomic DNA extracted from positive clones were backcrossed into the parental strain used for
520 the transposon screen. Transposon insertion sites were identified by inverse PCR using gDNA
521 extracted from the backcrossed positive clones (74) and sequencing the resulting PCR products.
522 Further verification of the transposon's site of insertion was obtained using specific primers.
523 For the suppressor screen in *ponA pbpD pbpF* mutant background, we constructed strain AG141
524 (**Table 2**) which carries deletions of the three vegetative class A PBPs, *lacA* gene (74) and
525 pLOSS-P_{spac}-*ponA* (12). The transposon mutant library was screened on PAB agar supplemented
526 with $MgSO_4$ (10 mM), X-Gal and IPTG (1 mM) and white colonies selected. The strain SWA11a
527 (**Table 2**) had a transposon in *mprF* coding sequence which was verified using specific primers
528 oAG81-82 (**Table 3**).

529 A conditional lethal screen was also carried out in a *ponA pbpD pbpF mprF lacA* pLOSS-P_{spac}-
530 *ponA* strain (AG200, **Table 2**). Here the transposon mutant library was screened on NA and PAB
531 supplemented with X-Gal and IPTG (1mM). Blue colonies indicating plasmid stability were
532 selected. One mutant was isolated and its genomic DNA was backcrossed into AG200
533 background. The resulting blue forming AG200BK#42 strain (**Table 2**) was found to carry a
534 transposon in *gtaB*'s coding sequence using primers oAG165-166 (**Table 3**).

535 ***Spot growth assays***

536 Strains were grown in NB with 20 mM $MgSO_4$ at 30°C overnight. The cultures were then diluted
537 1:100 into fresh NB 10 mM $MgSO_4$ (or when applicable 20 mM) and grown up to mid
538 exponential phase at 37°C. Cells were harvested, washed in NB, and diluted to an $OD_{600nm} \approx 0.3$
539 in NB. Each strain sample was then serially diluted 1:10 using a 96-multiwell plate and NB.
540 Using a multichannel pipette, 5 µl of each dilution were transferred to various agar plates. As a
541 control all the serial dilutions presented in the figures were also spotted on media supplemented
542 with 10 mM or 20 mM $MgS0_4$ to ensure that growth occurred for all spots (data not shown).
543 Plates were incubated at 37°C overnight and scanned at different time points. Images were edited
544 in Photoshop CS software.

545 ***Microscopic imaging***

546 Cells were grown to exponential growth phase at 37 °C in NB medium. Before the cells were
547 mounted onto microscopic slides, the slides were covered with a thin layer of NA medium
548 supplemented with the FM5-95 membrane dye at 140 µg/ml (Invitrogen). Fluorescence
549 microscopy was carried out with a Zeiss Axiovert 200M microscope attached to a Sony Cool-
550 Snap HQ cooled CCD camera with Nikon APO x100/1.40 oil Ph3 objective lens. Images were
551 acquired using Metamorph 6 imaging software (Molecular Devices, Inc). Images were analysed
552 with ImageJ (http://rsb.info.nih.gov/ij/) and assembled with Photoshop CS software.
553 Images stained with the FM5-95 membrane dye were processed using the plugin ObjectJ in
554 ImageJ (http://rsb.info.nih.gov/ij/) to measure cell diameter and cell length of about 400 cells per
555 strain. Measurements were performed only once as cell diameter change was obvious under the
556 microscope and on the images of **Fig 3D** (details in **Fig S3AB, Table 4**).

557 ***Transmission electron microscopy***

558 Strains were grown in NB medium (with IPTG when applicable) until reaching an OD_{600nm} of
559 about 0.4. The cell pellets were fixed in 2% glutaraldehyde in sodium cacodylate buffer at 4°C
560 for at least 24 h. Samples were spun and molten 4% agarose was added to the sample and re
561 spun. Sample were allowed to cool in the fridge for 30 min. The agarose block was removed
562 from each tube and cut into 1 mm^3 pieces. The samples were then dehydrated by microwave
563 processing using the Pelco Biowave® Pro+ incorporating the Pelco Coldspot® Pro. In the
564 vacuum chamber, samples were rinsed 3 times in buffer (150 watts for 40s), then treated in 1%
565 osmium, pulsed (100 watts for 8 min) and rinsed 3 times in distilled water (150 watts for 40s).
566 They were then taken out of the vaccum chamber and a graded series of dried acetone was
567 applied to the samples (25%, 50%,75%, and 3 times in 100%, at 150 watts for 40 s for each
568 step). This was followed by impregnation with a series of increasing concentrations of epoxy
569 resin (Taab Medium resin) in acetone (25%, 50%,75%, 3 times in 100% at 300 watts for 3 min.
570 for each step). Samples were embedded in fresh 100% resin and polymerised at 60°C for 24 h in
571 a conventional oven. Once polymerised the resin block were cut in semi-thin survey sections (0.5
572 μm) and stained with 1% toluidine blue in 1% borax. Ultrathin sections (70 nm approx.) were
573 then cut using a diamond knife on a Leica EM UC7 ultramicrotome. The sections were stretched
574 with chloroform to eliminate compression and mounted on Pioloform-filmed copper grids. Grids
575 were stained with uranyl acetate (2%) and Lead citrate and viewed on a Hitachi HT7800
576 transmission electron microscope using an Emsis Xarosa camera.

577 ***Samples preparation for LTA polymer detection***

578 *B. subtilis* strains were grown overnight at 30°C with shaking in NB supplemented with 5 mM
579 $MgS0_4$ (or 10 mM for *mbl* mutants). The cells were then diluted (1:60-1:80 depending on the
580 strain) to an approximate OD_{600nm} of 0.02 in prewarmed NB and NB supplemented with 0.2%
581 glucose. Strains were then incubated at 37°C shaking and grown for about 4.5 h (late exponential
582 phase). At the sampling time the OD_{600nm} of the cultures were measured before harvesting 15-25
583 ml of culture at 3273 *g* for 10 min, using a swing out centrifuge at room temperature. Pellets
584 were washed with 200 µl of solution A (with 10 mL of Tris-HCl at 100 mM pH 7.4 and one
585 cOmplete Mini EDTA-free tablet of protease inhibitor cocktail from Roche) and pelleted with
586 benchtop centrifuge. Cells pellets were then frozen in liquid nitrogen and stored at -20°C until
587 processing. Samples were resuspended in a volume of solution B (an equal volume of solution A
588 and LDS sample buffer, Life Technologies) ranging from 70 to 200 µl in proportion to their
589 OD_{600nm}. Samples were boiled 30 min at 100°C, cooled down on ice for 3 min and incubated
590 each with 100 U of benzonase (E1014, Sigma) for 30 min at 37°C. Samples were pelleted at 4°C,
591 supernatants containing the extracted LTA were collected. Supernatants were frozen in liquid
592 nitrogen and kept at -25°C. For the LTA Western blots, the quantity of sample loaded was
593 normalized using the Bio-Rad Protein assays such that the final OD_{595nm} was approximately 0.35.
594 Sample sets to be compared were grown, extracted, measured and normalized together for each
595 experiment.

596 *S. aureus* strains were grown overnight at 37°C with shaking in LB. The cells were then diluted
597 (about 300-fold) to an approximate OD_{600nm} of about 0.02 and grown in LB at 37°C until
598 reaching late exponential and an OD_{600nm} of about 1. 10 ml of cultures were harvested, and
599 samples were prepared as for *B. subtilis* with the following changes: 60 µl of solution B were

600 used and about 18-20 µl of samples were loaded on SDS-PAGE with samples normalised to their
601 OD_{600nm}.

602 ***Total protein samples preparation***

603 For LytE or LtaS Western blots, cells were grown, harvested and processed in the same way as
604 the LTA-samples, with the exception that to detect the His tagged proteins (LytE, LtaS or YfnI)
605 the strains were grown in presence of erythromycin. An 8 ml culture sample was resuspended in
606 180-200 µl of a solution A and sonicated until a clear lysate was obtained. Samples were
607 centrifuged at 16,000 *g* for 10 min at 4°C and a volume of sample supernatant loaded on the
608 SDS-gel, normalized based on the OD_{600nm} of the cells culture collected.

609 ***SDS-PAGE, LTA and proteins Western blots, detection blots***

610 For SDS-PAGE, samples were diluted in solution B with the addition of reducing agent (1.5 µl
611 per sample) in final volume of 20 µl, heated at 70°C for 10 min, loaded on the gel (NuPAGE 4-
612 12% Bis-Tris gradient Midi Gel, Life Technologies) and separated by electrophoresis. For the
613 LTA-PBP2B experiment, MES buffer, Novex Sharp prestained protein Ladder (Life
614 Technologies) and 0.2 µm Amersham Hybond sequencing PVDF membrane (GE Healthcare)
615 were used. Whereas for LytE (37 kDa) or LtaS (74 kDa) Western blots, MOPS buffer, Abcam
616 prestained mid-range protein ladder (Ab116027) and 0.45 µM Amersham Hybond PVDF
617 membrane (GE Healthcare) were used. The SDS-PAGE gels were transferred to membranes
618 using the Trans-Blot Turbo transfer system (Bio-Rad) using an in-house transfer buffer (tris 600
619 mM, glycine 600 mM, tricine 280 mM, EDTA 2.5 mM and SDS 0.05%). After transfer, the

620 membranes were washed 3x 5 min in PBS using a rocking shaker, afterwards the membranes
621 were cut where required to allow different detection methods.
622 For the LTA Western blot, membrane was cut at the 60 kDa ladder position. The bottom part of
623 the membrane was used for the LTA-blot whereas the top part was used to detect the membrane
624 protein PBP2B (79 kDa) as a loading/extraction control. All LTA Western blot steps were
625 performed at room temperature in a rolling shaker and using 50 mL falcon tubes. The LTA-
626 membranes were incubated 1h15 in PBS buffer with 3% BSA (A7030, Sigma), then 1h30 in
627 fresh PBS-3% BSA with a dilution 1:1000 of Gram-positive LTA monoclonal antibody (MA1-
628 7402, Thermofischer). The membrane was then washed briefly 2 times, followed by 4x 8 min in
629 PBS and then incubated in PBS-5% dried semi-skimmed milk with 1:10,000 anti-mouse HRP-
630 linked secondary antibody (A9044, Sigma) for 1 h. This was then followed by 2 brief and 6x 8
631 min washes steps prior to detection.
632 For proteins Western blots to detect LytE-His_{12} or LtaS and PBP2B, all the following steps were
633 performed at room temperature using a rocking shaker. The membranes were washed after
634 transfer in PBS-Tween20 at 0.1% (here after noted PBS-T) and blocked in PBS-T with 5% milk
635 for 1h15 (i.e PBS-T-milk) at room temperature. Thereafter the LytE-His_{12}/PBP2B membrane
636 blot was cut at about 53 kDa ladder position. Membranes were placed in fresh buffer PBS-T-
637 milk for 1h (or 1h30 when performing the LTAs western blot in parallel) with the polyclonal
638 rabbit anti-PBP2B antibody (at 1:5000, lab. stock or available at Merck ABS2199), the mouse
639 monoclonal Penta-His antibody (Qiagen n°34660 stock at 200 µg/ml, used at dilution 1:2000) or
640 polyclonal rabbit anti-LtaS antibody (at 1:1000, lab. stock). Two brief washing steps were
641 performed in PBS-T followed by 3 washes of 10 min. Membranes were incubated in PBS-T-milk
642 for 1 h using 1:10000 dilutions of anti-rabbit or anti-mouse HRP-linked secondary antibodies

643 (A0545 or A9044 Sigma antibodies, respectively) as required. Membranes were then washed as
644 described at the previous step.
645 Pierce ECL Plus Western Blotting Substrate (32132, Thermo Scientific) was used for detection
646 as recommended by manufacturer. Chemiluminescence was detected using ImageQuant LAS
647 4000 mini digital imaging system (GE Healthcare) and membranes were exposed with 1 min
648 increment for 20 min. Membranes were also imaged by Epi-illumination to detect the pre-stained
649 proteins ladder on the membrane. In our conditions, quantities of LTAs samples loaded were
650 scaled down to avoid burn out of signals observed in some of the tested strains. Occasionally for
651 the LTAs blot, strains (in NB-only) can display a very weak signal above the 30 kDa ladder
652 position. This phenomenon was observed by others performing *Bacillus* LTA Western blots and
653 was assumed not to be related to LTA but possibly a cross-reactivity of the antibody to WTAs
654 that also contains glycerolphosphate (18).
655 Images were edited in ImageJ (Fiji), the same contrast enhancement was applied for the
656 membranes of the same set experiment. Three independent sets of experimental samples were
657 generated by Western blots. Contrast was sometimes added to the images, in particular to
658 observe LytE signal in low-expressing strains.

659 ***LytE purification and raising antiserum***

660 Plasmid pAM-21 was transferred into *E. coli* BL21 (DE3) strain. Newly obtained strain grew at
661 37°C in LB kanamycin, when cell reached an approximative OD_{600nm} of 0.5 *lytE* expression was
662 induced with 1 mM IPTG for 3 h. 50 ml culture was collected by centrifugation at 9,000 *g* for 5
663 min and resuspended in 15 ml of a solution of PBS at 4 µg/ml of lysosyme. After incubation for
664 20 min at room temperature (RT), cells were sonicated, and once clear lysate was obtained cells

665 were harvested at 3,000 *g* for 4 min. The cell pellet was resuspended in PBS buffer at 8 M Urea
666 and incubated for 30 min at RT on a rolling shaker. The cells were then centrifuged at 9,000 *g*
667 for 10 min and supernatant was collected and mixed gently with 200 µl of Ni Sepharose High
668 Performance (GE Healthcare) and incubated for 1 h in same condition as above. Then the sample
669 was washed 3 to 4 times in buffer A (50 mM Tris (pH 8) and 300 mM NaCl), and the last wash
670 was done in buffer B (50 mM Tris, 300 mM NaCl, 5 mM Imidazole). Sample was eluted five
671 times in buffer C (PBS at 8 M Urea and 100 mM imidazole) and elution fractions were analysed
672 by SDS-PAGE. Ice-cold acetone was added at a 4:1 volume ratio to the desired eluted sample
673 and incubated overnight at -20°C. Sample was centrifuged at 4 °C for 10 min at 15,000 *g* and the
674 pellet was left to dry at RT. The pellet was suspended in 200 µl of PBS and 100 µg aliquot was
675 sent to raise antiserum (Eurogentec). The LytE antiserum was used in Western blot at 1:5000
676 dilution and with the anti-rabbit secondary antibody (1:10000).

677 ***Growth assays in presence of Daptomycin***

678 For the *S. aureus* samples for LTA Western blot, cultures were done as previously described but
679 after 3h growing in LB, $CaCl_2$ (1.25 mM final) was added to the cultures which were then
680 divided and grown an extra hour with or without daptomycin (Dap stock at 1 mg/ml, Abcam
681 ab141204).

682 For the NA-$CaCl_2$ DAP assays, strains were exponentially growing in NB for about 3h at 37°C
683 (exponential phase) and then normalized to an OD_{600nm} of 0.5. Cells (300 µl) were spread on
684 calibrated NA plate supplemented with $CaCl_2$ (1.25 mM final). A daptomycin 0.016-256 mg/l
685 antimicrobial susceptibility testing strip (Liofilchem) was applied to the medium surface. Plates

686 were incubated at 37°C overnight and scanned after 24h. Images were edited in Fiji (ImageJ).
687 Interpretation on growth inhibition follows manufacturer's guidance.
688 To monitor strain growth in a plate reader, we used pre-cultures which has grown in NB (or in
689 LB for *S. aureus*) at 37°C for about 3h. For each assays, a daptomycin stock at 17.4 mg/ml was
690 used to prepare a fresh DAP stock at 0.1 mg/ml and this was used to make dilutions of the
691 antibiotic as required in 96-wells plates in 100 µl of medium supplemented with $CaCl_2$ (1.25mM
692 final). Plates were then loaded with 100 µl of cells (diluted in medium-$CaCl_2$ and normalized at
693 the desired OD_{600nm}). Plates were shaken at 37°C in a Tecan Sunrise plate reader and the OD_{600nm}
694 was measured every 6 min. Conditions were tested in duplicate or triplicates whenever possible.
695 Data were collected using Magellan software (version 7.2). Microsoft Excel was used for
696 analysis and generating graphs.

Acknowledgements

The authors thank P. Aldridge for critical reading of the manuscript. The authors thank colleagues for strains, genomic DNAs or daptomycin stock: S. Moore, P. Dominguez-Cuevas, P. Gamba, A. Koh, K. Seistrup, L. Bowman, J. Buttress, H. Strahl and J. D. Helmann, B. M. Wendel and A. Peschel for strains related to daptomycin resistance. Technical support was provided by I. Selmes, F. Davison and T. Fletcher and TEM sample processing by Tracey Davey in the Electron Microscopy Research Services Newcastle University (funded through the BBSRC; BB/R013942/1). The authors thank J. Errington for the anti-LtaS antibody, H. Strahl and W. Vollmer for helpful discussion, C. Winterhalter and S. Fenyk for advice on Western blots and P. Tiago for sharing subtiwiki data. This work was funded by grants from the BBSRC (BB/G015902/1), EPSRC (EP/N031962/1) (RAD and AG) and SACB (studentship for AA).

Author contributions

Conceptualization: AG; Funding acquisition, RAD; Methodology: AG; Investigation: AG and AA; Methodology: AG; Project administration: RAD; Supervision: RAD; Validation: AG; Visualization: AG; Writing—original draft: AG; Writing—review & editing: AG and RAD.

Conflict of interest

The authors declare that they have no conflict of interest.

Supporting information

Figures, Tables and Supplemental Figures are available for this manuscript. This study includes no data deposited in external repositories.

717 **References**

718 1. Hanson BR, Neely MN. 2012. Coordinate regulation of Gram-positive cell surface
719 components. Curr Opin Microbiol 15:204-10.
720 2. Percy MG, Grundling A. 2014. Lipoteichoic Acid Synthesis and Function in Gram-
721 Positive Bacteria. Annu Rev Microbiol doi:10.1146/annurev-micro-091213-112949.
722 3. Schneewind O, Missiakas D. 2016. Lipoteichoic acid synthesis and function in gram-
723 positive bacteria. Biogenesis of Fatty Acids, Lipids and Membranes:1-18.
724 4. Rajagopal M, Walker S. 2017. Envelope Structures of Gram-Positive Bacteria. Curr Top
725 Microbiol Immunol 404:1-44.
726 5. Neuhaus FC, Baddiley J. 2003. A continuum of anionic charge: structures and functions
727 of D-alanyl-teichoic acids in Gram-positive bacteria. Microbiol Mol Biol Rev 67:686-
728 723.
729 6. Erickson HP. 2021. How Teichoic Acids Could Support a Periplasm in Gram-Positive
730 Bacteria, and Let Cell Division Cheat Turgor Pressure. Front Microbiol 12:664704.
731 7. Pazos M, Vollmer W. 2021. Regulation and function of class A Penicillin-binding
732 proteins. Curr Opin Microbiol 60:80-87.
733 8. Straume D, Piechowiak KW, Kjos M, Havarstein LS. 2021. Class A PBPs: It is time to
734 rethink traditional paradigms. Mol Microbiol doi:10.1111/mmi.14714.
735 9. McPherson DC, Popham DL. 2003. Peptidoglycan synthesis in the absence of class A
736 penicillin-binding proteins in *Bacillus subtilis*. J Bacteriol 185:1423-31.
737 10. Kawai Y, Daniel RA, Errington J. 2009. Regulation of cell wall morphogenesis in
738 *Bacillus subtilis* by recruitment of PBP1 to the MreB helix. Mol Microbiol 71:1131-44.
739 11. Meeske AJ, Riley EP, Robins WP, Uehara T, Mekalanos JJ, Kahne D, Walker S, Kruse
740 AC, Bernhardt TG, Rudner DZ. 2016. SEDS proteins are a widespread family of
741 bacterial cell wall polymerases. Nature 537:634-638.
742 12. Emami K, Guyet A, Kawai Y, Devi J, Wu LJ, Allenby N, Daniel RA, Errington J. 2017.
743 RodA as the missing glycosyltransferase in *Bacillus subtilis* and antibiotic discovery for
744 the peptidoglycan polymerase pathway. Nat Microbiol 2:16253.
745 13. Do T, Page JE, Walker S. 2020. Uncovering the activities, biological roles, and
746 regulation of bacterial cell wall hydrolases and tailoring enzymes. J Biol Chem 295:3347-
747 3361.

748 14. Wilson S, Garner E. 2021. An Exhaustive Multiple Knockout Approach to Understanding
749 Cell Wall Hydrolase Function in *Bacillus subtilis*. bioRxiv
750 doi:10.1101/2021.02.18.431929:2021.02.18.431929.
751 15. Brunet YR, Wang X, Rudner DZ. 2019. SweC and SweD are essential co-factors of the
752 FtsEX-CwlO cell wall hydrolase complex in *Bacillus subtilis*. PLoS Genet 15:e1008296.
753 16. Schirner K, Marles-Wright J, Lewis RJ, Errington J. 2009. Distinct and essential
754 morphogenic functions for wall- and lipo-teichoic acids in *Bacillus subtilis*. EMBO J
755 28:830-42.
756 17. Soldo B, Lazarevic V, Karamata D. 2002. *tagO* is involved in the synthesis of all anionic
757 cell-wall polymers in *Bacillus subtilis* 168. Microbiology (Reading) 148:2079-2087.
758 18. Wormann ME, Corrigan RM, Simpson PJ, Matthews SJ, Grundling A. 2011. Enzymatic
759 activities and functional interdependencies of *Bacillus subtilis* lipoteichoic acid synthesis
760 enzymes. Mol Microbiol 79:566-83.
761 19. Schneewind O, Missiakas D. 2014. Lipoteichoic acids, phosphate-containing polymers in
762 the envelope of Gram-positive bacteria. J Bacteriol 196:1133-42.
763 20. Kingston AW, Liao X, Helmann JD. 2013. Contributions of the σ^W , σ^M and σ^X regulons
764 to the lantibiotic resistome of *Bacillus subtilis*. Mol Microbiol 90:502-18.
765 21. Peschel A, Jack RW, Otto M, Collins LV, Staubitz P, Nicholson G, Kalbacher H,
766 Nieuwenhuizen WF, Jung G, Tarkowski A, van Kessel KP, van Strijp JA. 2001.
767 *Staphylococcus aureus* resistance to human defensins and evasion of neutrophil killing
768 via the novel virulence factor MprF is based on modification of membrane lipids with l-
769 lysine. J Exp Med 193:1067-76.
770 22. Slavetinsky C, Kuhn S, Peschel A. 2017. Bacterial aminoacyl phospholipids -
771 Biosynthesis and role in basic cellular processes and pathogenicity. Biochim Biophys
772 Acta Mol Cell Biol Lipids 1862:1310-1318.
773 23. Staubitz P, Peschel A. 2002. MprF-mediated lysinylation of phospholipids in *Bacillus*
774 *subtilis* - protection against bacteriocins in terrestrial habitats? Microbiology 148:3331-2.
775 24. Johnson CM, Grossman AD. 2016. The Composition of the Cell Envelope Affects
776 Conjugation in *Bacillus subtilis*. J Bacteriol 198:1241-9.

777 25. Atila M, Katselis G, Chumala P, Luo Y. 2016. Characterization of N-Succinylation of L-
778 Lysylphosphatidylglycerol in *Bacillus subtilis* Using Tandem Mass Spectrometry. J Am
779 Soc Mass Spectrom 27:1606-13.
780 26. Ernst CM, Peschel A. 2019. MprF-mediated daptomycin resistance. Int J Med Microbiol
781 309:359-363.
782 27. Nowak J, Visnovsky SB, Cruz CD, Fletcher GC, van Vliet AHM, Hedderley D, Butler R,
783 Flint S, Palmer J, Pitman AR. 2021. Inactivation of the gene encoding the cationic
784 antimicrobial peptide resistance factor MprF increases biofilm formation but reduces
785 invasiveness of *Listeria monocytogenes*. J Appl Microbiol 130:464-477.
786 28. Salzberg LI, Helmann JD. 2008. Phenotypic and transcriptomic characterization of
787 *Bacillus subtilis* mutants with grossly altered membrane composition. J Bacteriol
788 190:7797-807.
789 29. Hachmann AB, Angert ER, Helmann JD. 2009. Genetic analysis of factors affecting
790 susceptibility of *Bacillus subtilis* to daptomycin. Antimicrob Agents Chemother 53:1598-
791 609.
792 30. Jorasch P, Wolter FP, Zahringer U, Heinz E. 1998. A UDP glucosyltransferase from
793 *Bacillus subtilis* successively transfers up to four glucose residues to 1,2-diacylglycerol:
794 expression of *ypfP* in *Escherichia coli* and structural analysis of its reaction products.
795 Mol Microbiol 29:419-30.
796 31. Lazarevic V, Soldo B, Medico N, Pooley H, Bron S, Karamata D. 2005. *Bacillus subtilis*
797 α-phosphoglucomutase is required for normal cell morphology and biofilm formation.
798 Appl Environ Microbiol 71:39-45.
799 32. Grundling A, Schneewind O. 2007. Genes required for glycolipid synthesis and
800 lipoteichoic acid anchoring in *Staphylococcus aureus*. J Bacteriol 189:2521-30.
801 33. Hesser AR, Schaefer K, Lee W, Walker S. 2020. Lipoteichoic acid polymer length is
802 determined by competition between free starter units. Proc Natl Acad Sci U S A
803 117:29669-29676.
804 34. Oku Y, Kurokawa K, Matsuo M, Yamada S, Lee BL, Sekimizu K. 2009. Pleiotropic roles
805 of polyglycerolphosphate synthase of lipoteichoic acid in growth of *Staphylococcus*
806 *aureus* cells. J Bacteriol 191:141-51.

807 35. Coe KA, Lee W, Stone MC, Komazin-Meredith G, Meredith TC, Grad YH, Walker S.
808 2019. Multi-strain Tn-Seq reveals common daptomycin resistance determinants in
809 *Staphylococcus aureus*. PLoS Pathog 15:e1007862.
810 36. Grundling A, Schneewind O. 2007. Synthesis of glycerol phosphate lipoteichoic acid in
811 *Staphylococcus aureus*. Proc Natl Acad Sci U S A 104:8478-83.
812 37. Hashimoto M, Seki T, Matsuoka S, Hara H, Asai K, Sadaie Y, Matsumoto K. 2013.
813 Induction of extracytoplasmic function sigma factors in *Bacillus subtilis* cells with
814 defects in lipoteichoic acid synthesis. Microbiology 159:23-35.
815 38. Murray T, Popham DL, Setlow P. 1998. *Bacillus subtili*s cells lacking penicillin-binding
816 protein 1 require increased levels of divalent cations for growth. J Bacteriol 180:4555-63.
817 39. Claessen D, Emmins R, Hamoen LW, Daniel RA, Errington J, Edwards DH. 2008.
818 Control of the cell elongation-division cycle by shuttling of PBP1 protein in *Bacillus*
819 *subtilis*. Mol Microbiol 68:1029-46.
820 40. Perego M, Glaser P, Minutello A, Strauch MA, Leopold K, Fischer W. 1995.
821 Incorporation of D-alanine into lipoteichoic acid and wall teichoic acid in *Bacillus*
822 *subtilis*. Identification of genes and regulation. J Biol Chem 270:15598-606.
823 41. Wood BM, Santa Maria JP, Jr., Matano LM, Vickery CR, Walker S. 2018. A partial
824 reconstitution implicates DltD in catalyzing lipoteichoic acid d-alanylation. J Biol Chem
825 293:17985-17996.
826 42. Kawai Y, Asai K, Errington J. 2009. Partial functional redundancy of MreB isoforms,
827 MreB, Mbl and MreBH, in cell morphogenesis of *Bacillus subtilis*. Mol Microbiol
828 73:719-31.
829 43. Dominguez-Cuevas P, Porcelli I, Daniel RA, Errington J. 2013. Differentiated roles for
830 MreB-actin isologues and autolytic enzymes in *Bacillus subtilis* morphogenesis. Mol
831 Microbiol 89:1084-98.
832 44. Hashimoto M, Ooiwa S, Sekiguchi J. 2012. Synthetic lethality of the *lytE cwlO* genotype
833 in *Bacillus subtilis* is caused by lack of D,L-endopeptidase activity at the lateral cell wall.
834 J Bacteriol 194:796-803.
835 45. Salzberg LI, Powell L, Hokamp K, Botella E, Noone D, Devine KM. 2013. The WalRK
836 (YycFG) and σ^I RsgI regulators cooperate to control CwlO and LytE expression in
837 exponentially growing and stressed *Bacillus subtilis* cells. Mol Microbiol 87:180-95.

838 46. Dobihal GS, Brunet YR, Flores-Kim J, Rudner DZ. 2019. Homeostatic control of cell
839 wall hydrolysis by the WalRK two-component signaling pathway in *Bacillus subtilis*.
840 Elife 8.
841 47. Kasahara J, Kiriyama Y, Miyashita M, Kondo T, Yamada T, Yazawa K, Yoshikawa R,
842 Yamamoto H. 2016. Teichoic Acid Polymers Affect Expression and Localization of dl-
843 Endopeptidase LytE Required for Lateral Cell Wall Hydrolysis in *Bacillus subtilis*. J
844 Bacteriol 198:1585-1594.
845 48. Mamou G, Fiyaksel O, Sinai L, Ben-Yehuda S. 2017. Deficiency in Lipoteichoic Acid
846 Synthesis Causes a Failure in Executing the Colony Developmental Program in *Bacillus*
847 *subtilis*. Front Microbiol 8:1991.
848 49. Muller A, Wenzel M, Strahl H, Grein F, Saaki TNV, Kohl B, Siersma T, Bandow JE,
849 Sahl HG, Schneider T, Hamoen LW. 2016. Daptomycin inhibits cell envelope synthesis
850 by interfering with fluid membrane microdomains. Proc Natl Acad Sci U S A 113:E7077-
851 E7086.
852 50. Gray DA, Wenzel M. 2020. More Than a Pore: A Current Perspective on the In Vivo
853 Mode of Action of the Lipopeptide Antibiotic Daptomycin. Antibiotics (Basel) 9.
854 51. Grein F, Muller A, Scherer KM, Liu X, Ludwig KC, Klockner A, Strach M, Sahl HG,
855 Kubitscheck U, Schneider T. 2020. Ca^{2+}-Daptomycin targets cell wall biosynthesis by
856 forming a tripartite complex with undecaprenyl-coupled intermediates and membrane
857 lipids. Nat Commun 11:1455.
858 52. Friedman L, Alder JD, Silverman JA. 2006. Genetic changes that correlate with reduced
859 susceptibility to daptomycin in *Staphylococcus aureus*. Antimicrob Agents Chemother
860 50:2137-45.
861 53. Ernst CM, Slavetinsky CJ, Kuhn S, Hauser JN, Nega M, Mishra NN, Gekeler C, Bayer
862 AS, Peschel A. 2018. Gain-of-Function Mutations in the Phospholipid Flippase MprF
863 Confer Specific Daptomycin Resistance. mBio 9.
864 54. Hachmann AB, Sevim E, Gaballa A, Popham DL, Antelmann H, Helmann JD. 2011.
865 Reduction in membrane phosphatidylglycerol content leads to daptomycin resistance in
866 *Bacillus subtilis*. Antimicrob Agents Chemother 55:4326-37.
867 55. Hesser AR, Matano LM, Vickery CR, Wood BM, Santiago AG, Morris HG, Do T,
868 Losick R, Walker S. 2020. The length of lipoteichoic acid polymers controls

869 *Staphylococcus aureus* cell size and envelope integrity. J Bacteriol
870 doi:10.1128/JB.00149-20.
871 56. Flores-Kim J, Dobihal GS, Fenton A, Rudner DZ, Bernhardt TG. 2019. A switch in
872 surface polymer biogenesis triggers growth-phase-dependent and antibiotic-induced
873 bacteriolysis. Elife 8.
874 57. Patel Y, Zhao H, Helmann JD. 2020. A regulatory pathway that selectively up-regulates
875 elongasome function in the absence of class A PBPs. Elife 9.
876 58. Nicolas P, Mader U, Dervyn E, Rochat T, Leduc A, Pigeonneau N, Bidnenko E,
877 Marchadier E, Hoebeke M, Aymerich S, Becher D, Bisicchia P, Botella E, Delumeau O,
878 Doherty G, Denham EL, Fogg MJ, Fromion V, Goelzer A, Hansen A, Hartig E, Harwood
879 CR, Homuth G, Jarmer H, Jules M, Klipp E, Le Chat L, Lecointe F, Lewis P,
880 Liebermeister W, March A, Mars RA, Nannapaneni P, Noone D, Pohl S, Rinn B,
881 Rugheimer F, Sappa PK, Samson F, Schaffer M, Schwikowski B, Steil L, Stulke J,
882 Wiegert T, Devine KM, Wilkinson AJ, van Dijl JM, Hecker M, Volker U, Bessieres P, et
883 al. 2012. Condition-dependent transcriptome reveals high-level regulatory architecture in
884 *Bacillus subtilis*. Science 335:1103-6.
885 59. Zhu B, Stulke J. 2018. SubtiWiki in 2018: from genes and proteins to functional network
886 annotation of the model organism *Bacillus subtilis*. Nucleic Acids Res 46:D743-D748.
887 60. Wendel BM, Pi H, Kruger L, Herzberg C, Stulke J, Helmann JD. 2022. A Central Role
888 for Magnesium Homeostasis during Adaptation to Osmotic Stress. mBio
889 doi:10.1128/mbio.00092-22:e0009222.
890 61. Tesson B, Dajkovic A, Keary R, Marliere C, Dupont-Gillain CC, Carballido-Lopez R.
891 2022. Magnesium rescues the morphology of *Bacillus subtilis mreB* mutants through its
892 inhibitory effect on peptidoglycan hydrolases. Sci Rep 12:1137.
893 62. Song D, Jiao H, Liu Z. 2021. Phospholipid translocation captured in a bifunctional
894 membrane protein MprF. Nat Commun 12:2927.
895 63. Joyce LR, Manzer HS, da CMJ, Villarreal R, Nagao PE, Doran KS, Palmer KL, Guan Z.
896 2022. Identification of a novel cationic glycolipid in *Streptococcus agalactiae* that
897 contributes to brain entry and meningitis. PLoS Biol 20:e3001555.
898 64. Thitiananpakorn K, Aiba Y, Tan XE, Watanabe S, Kiga K, Sato'o Y, Boonsiri T, Li FY,
899 Sasahara T, Taki Y, Azam AH, Zhang Y, Cui L. 2020. Association of *mprF* mutations

900 with cross-resistance to daptomycin and vancomycin in methicillin-resistant
901 *Staphylococcus aureus* (MRSA). Sci Rep 10:16107.
902 65. Bertsche U, Yang SJ, Kuehner D, Wanner S, Mishra NN, Roth T, Nega M, Schneider A,
903 Mayer C, Grau T, Bayer AS, Weidenmaier C. 2013. Increased cell wall teichoic acid
904 production and D-alanylation are common phenotypes among daptomycin-resistant
905 methicillin-resistant *Staphylococcus aureus* (MRSA) clinical isolates. PLoS One
906 8:e67398.
907 66. Mishra NN, Bayer AS, Weidenmaier C, Grau T, Wanner S, Stefani S, Cafiso V,
908 Bertuccio T, Yeaman MR, Nast CC, Yang SJ. 2014. Phenotypic and genotypic
909 characterization of daptomycin-resistant methicillin-resistant *Staphylococcus aureus*
910 strains: relative roles of *mprF* and *dlt* operons. PLoS One 9:e107426.
911 67. Yang SJ, Nast CC, Mishra NN, Yeaman MR, Fey PD, Bayer AS. 2010. Cell wall
912 thickening is not a universal accompaniment of the daptomycin nonsusceptibility
913 phenotype in *Staphylococcus aureus*: evidence for multiple resistance mechanisms.
914 Antimicrob Agents Chemother 54:3079-85.
915 68. Muscato JD, Morris HG, Mychack A, Rajagopal M, Baidin V, Hesser AR, Lee W, Inecik
916 K, Wilson LJ, Kraml CM, Meredith TC, Walker S. 2022. Rapid Inhibitor Discovery by
917 Exploiting Synthetic Lethality. J Am Chem Soc 144:3696-3705.
918 69. Chee Wezen X, Chandran A, Eapen RS, Waters E, Bricio-Moreno L, Tosi T, Dolan S,
919 Millership C, Kadioglu A, Grundling A, Itzhaki LS, Welch M, Rahman T. 2022.
920 Structure-Based Discovery of Lipoteichoic Acid Synthase Inhibitors. J Chem Inf Model
921 62:2586-2599.
922 70. Slavetinsky CJ, Hauser JN, Gekeler C, Slavetinsky J, Geyer A, Kraus A, Heilingbrunner
923 D, Wagner S, Tesar M, Krismer B, Kuhn S, Ernst CM, Peschel A. 2022. Sensitizing
924 *Staphylococcus aureus* to antibacterial agents by decoding and blocking the lipid flippase
925 MprF. Elife 11.
926 71. Anagnostopoulos C, Spizizen J. 1961. Requirements for Transformation in *Bacillus*
927 *subtilis*. J Bacteriol 81:741-6.
928 72. Hamoen LW, Smits WK, de Jong A, Holsappel S, Kuipers OP. 2002. Improving the
929 predictive value of the competence transcription factor (ComK) binding site in *Bacillus*
930 *subtilis* using a genomic approach. Nucleic Acids Res 30:5517-28.

931 73. Ishikawa S, Kawai Y, Hiramatsu K, Kuwano M, Ogasawara N. 2006. A new FtsZ-
932 interacting protein, YlmF, complements the activity of FtsA during progression of cell
933 division in *Bacillus subtilis*. Mol Microbiol 60:1364-80.
934 74. Surdova K, Gamba P, Claessen D, Siersma T, Jonker MJ, Errington J, Hamoen LW.
935 2013. The conserved DNA-binding protein WhiA is involved in cell division in *Bacillus*
936 *subtilis*. J Bacteriol 195:5450-60.
937 75. Veening JW, Kuipers OP, Brul S, Hellingwerf KJ, Kort R. 2006. Effects of phosphorelay
938 perturbations on architecture, sporulation, and spore resistance in biofilms of *Bacillus*
939 *subtilis*. J Bacteriol 188:3099-109.
940 76. Steinmetz M, Richter R. 1994. Plasmids designed to alter the antibiotic resistance
941 expressed by insertion mutations in *Bacillus subtilis*, through in vivo recombination.
942 Gene 142:79-83.
943 77. Le Breton Y, Mohapatra NP, Haldenwang WG. 2006. *In vivo* random mutagenesis of
944 *Bacillus subtilis* by use of TnYLB-1, a mariner-based transposon. Appl Environ
945 Microbiol 72:327-33.
946 78. Formstone A, Errington J. 2005. A magnesium-dependent *mreB* null mutant: implications
947 for the role of *mreB* in *Bacillus subtilis*. Mol Microbiol 55:1646-57.
948 79. Schirner K, Errington J. 2009. The cell wall regulator σ^I specifically suppresses the lethal
949 phenotype of *mbl* mutants in *Bacillus subtilis*. J Bacteriol 191:1404-13.
950 80. McPherson DC, Driks A, Popham DL. 2001. Two class A high-molecular-weight
951 penicillin-binding proteins of *Bacillus subtilis* play redundant roles in sporulation. J
952 Bacteriol 183:6046-53.
953 81. Branda SS, Gonzalez-Pastor JE, Dervyn E, Ehrlich SD, Losick R, Kolter R. 2004. Genes
954 involved in formation of structured multicellular communities by *Bacillus subtilis*. J
955 Bacteriol 186:3970-9.
956 82. Koo BM, Kritikos G, Farelli JD, Todor H, Tong K, Kimsey H, Wapinski I, Galardini M,
957 Cabal A, Peters JM, Hachmann AB, Rudner DZ, Allen KN, Typas A, Gross CA. 2017.
958 Construction and Analysis of Two Genome-Scale Deletion Libraries for *Bacillus subtilis*.
959 Cell Syst 4:291-305 e7.

960 83. Matsuoka S, Hashimoto M, Kamiya Y, Miyazawa T, Ishikawa K, Hara H, Matsumoto K.
961 2011. The *Bacillus subtilis* essential gene *dgkB* is dispensable in mutants with defective
962 lipoteichoic acid synthesis. Genes Genet Syst 86:365-76.
963

964 **TABLE 1** Plasmids used in this study (by alphabetic order)

Plasmids	**Relevant features**[a]	**Source or reference**
pAM-21	*kan* P_{T7} LytE$^{(26\text{-}334AA)}$-6His *lacI*	This study
pCotC-GFP	used as matrix to amplify *cat*	(75)
pDR111	*bla amyE::(lacI* $P_{hyspank}$*, spc)*	Rudner, D., unpublished
pDR111-$P_{hyspank}$-*ltaS*	*bla amyE::(lacI* $P_{hyspank}$*-ltaS, spc)*	This study
pDR111-$P_{hyspank}$-*mprF*	*bla amyE::(lacI* $P_{hyspank\text{-}ATG}$*mprF, spc)*	This study
pDR111-$P_{hyspank}$-*yfnI*	*bla amyE::(lacI* $P_{hyspank}$*-yfnI, spc)*	This study
pDR111-$P_{hyspank}$-*yqgS*	*bla amyE::(lacI* $P_{hyspank}$*-yqgS, spc)*	This study
pET28a (+)	*kan* P_{T7} *his lacI*	Novagen
pG^{+}host9::*ΔponA*	*erm*, carry flanking DNA regions of *ponA*	(12)
pG^{+}host10::*ΔpbpD*	*bla*, carry flanking DNA regions of *pbpD*	(12)
pG^{+}host10::*ΔpbpF*	*bla*, carry flanking DNA regions of *pbpF*	(12)
pIC22	used as matrix to amplify *phleo*	(76)
pLOSS*	*bla spc* P_{spac}*-mcs* P_{divIVA}*-lacZ lacI* rep_{pLS20}*(GA→CC)*	(39)
pLOSS-P_{spac}-*lytE*	*bla spc* P_{spac}*-lytE* P_{divIVA}*-lacZ lacI* rep_{pLS20}*(GA→CC)*	This study
pLOSS-P_{spac}-*ponA*	*bla spc* P_{spac}*-ponA* P_{divIVA}*-lacZ lacI* rep_{pLS20}*(GA→CC)*	(12)
pMarB	*bla erm* TnYLB-1::*kan Himar1* transposase	(77)
pMUTinHis	*bla erm* P_{spac} *mcs 12xhis lacZ lacI*	(73)
pMUTin-`*lytE-his*	*bla erm* P_{spac} *mcs* `LytE-6AA-12His *lacZ lacI*	This study
pMUTin-`*ltaS-his*	*bla erm* P_{spac} *mcs* `LtaS-6AA-12His *lacZ lacI*	This study
pMUTin-`*yfnI-his*	*bla erm* P_{spac} *mcs* `YfnI-6AA-12His *lacZ lacI*	This study

965 [a]*cat,* chloramphenicol resistance; *bla*, ampicillin resistance; *spc*, spectinomycin resistance; *erm*,
966 erythromycin resistance; *phleo*, phleomycin resistance; *kan*, kanamycin resistance; *lacI*, encodes
967 lactose repressor; *mcs,* multiple cloning site; *lacZ*, encodes β-galactosidase; AA, amino acids;
968 $P_{hyspank}$ and P_{spac} are IPTG-inducible promoters with $P_{hyspank}$ known to be stronger;
969 rep_{pLS20}*(GA→CC)*, unstable replication in *Bacillus.*

970 **TABLE 2** Strains used in this study

Strains	**Relevant genotype**[a]	**Source or reference**[b]
E. coli		
DH5α	F^- endA1 glnV44 thi-1 recA1 relA1 gyrA96 deoR nupG Φ80d*lacZ*ΔM15 Δ(*lacZYA-argF*)U169, hsdR17(r_K^- m_K^+), λ–	Lab. stock
BL21(DE3)	B F^- *ompT gal dcm lon hsdS*$_B$(r_B^-*m*$_B^-$) λ(DE3 [*lacI lacUV5-T7p07 ind1 sam7 nin5*]) [*malB*$^+$]$_{K-12}$(λ^S)	Novagen
B. subtilis		
168CA	*trpC2*	R. Daniel Lab. stock
168 1A1	*trpC2* (BGSC n° 1A1)	(54)
3725CA	*trpC2 Ωneo ΔmreB*	3725 (78) → 168CA cells
4261CA	*trpC2 Δmbl::cat*	4261 (79) → 168CA cells
4283CA	*trpC2* Δ*ltaS::neo*	4283 (79) → 168CA cells
4285CA	*trpC2 ΔltaS::cat*	4285 (79) → 168CA cells
4287CA	*trpC2 ΔyfnI::spc*	4287 (79) → 168CA cells
4289CA	*trpC2 ΔyfnI::erm*	4289 (79) → 168CA cells
4292CA	*trpC2 ΔyqgS::spc*	4292 (79) → 168CA cells
4293CA	*trpC2* Δ*yqgS::cat*	4293 (79) → 168CA cells
4294CA	*trpC2* Δ*yqgS::erm*	4294 (79) → 168CA cells
4295CA	*trpC2 ΔyvgJ::spc*	4295 (79) → 168CA cells
4620	*trpC2* Δ*ltaS::neo* Δ*yfnI::cat* Δ*yqgS::spc* Δ*yvgJ::erm*	(79)
AG105	*trpC2 ΔpbpD ΔpbpF*	pGhost10::ΔpbpF (12) → RE103 cells
AG108	*trpC2 ΔponA ΔpbpD ΔpbpF*	pG$^+$host10::*ΔpbpF* → RE104 cells
AG123	*trpC2 ΔponA ΔpbpD ΔpbpF* pLOSS-P_{spac}-*ponA*	pLOSS-P_{spac}-*ponA* → AG108 cells
AG141	*trpC2 ΔponA ΔpbpD ΔpbpF* pLOSS-P_{spac}-*ponA lacA::cat*	K532 → AG123 cells
AG157	*trpC2 ΔponA ΔpbpD ΔpbpF ΔpbpG::kan*	(12)
AG181	*trpC2 ΔmprF::phleo*	This study
AG185	*trpC2 ΔmprF::phleo Ωneo ΔmreB*	3725CA → AG181 cells
AG189	*trpC2 ΔmprF::phleo Δmbl::cat*	4261CA → AG181 cell
AG193	*trpC2 ΔponA ΔmprF::phleo*	AG181 → RE101 cells
AG200	*trpC2 ΔponA ΔpbpD ΔpbpF* pLOSS-P_{spac}-*ponA ΔmprF::phleo lacA::cat*	AG181 → AG141 cells

AG200BK#42	*trpC2 ΔponA ΔpbpD ΔpbpF* pLOSS-P_{spac}-*ponA ΔmprF::phleo lacA::cat gtaB::*TnYLB-1*(kan)*	This study
AG210	*trpC2 ΔponA ΔpbpD ΔpbpF ΔpbpG::kan ΔmprF::phleo lacA::cat* pLOSS-P_{spac}-*ponA*	DPVB45CA → AG200 cells
AG211	*trpC2 ΔponA ΔpbpD ΔpbpF ΔpbpG::kan* pLOSS-P_{spac}-*ponA*	DPVB45CA → AG123 cells
AG223	*trpC2 ΔponA ΔpbpD ΔpbpF ΔpbpG::kan ΔmprF::phleo*	AG181 → AG157 cells
AG290	*trpC2 ΔponA ΔpbpD ΔpbpF ΔpbpG::kan* pLOSS-P_{spac}-*ponA ΔgtaB::erm*	SM08 → AG211 cells
AG290NopLoss	*trpC2 ΔponA ΔpbpD ΔpbpF ΔpbpG::kan ΔgtaB::erm*	AG290 lost plasmid on 20 mM $MgS0_4$ with kan
AG292	*trpC2 ΔponA ΔpbpD ΔpbpF ΔpbpG::kan* pLOSS-P_{spac}-*ponA Ωerm ΔtagE*	SM50 → AG211 cells
AG293	*trpC2 ΔponA ΔpbpD ΔpbpF ΔpbpG::kan ggaAB::spc*	SM31 → AG229 cells
AG296	*trpC2 ΔponA ΔpbpD ΔpbpF ΔpbpG::kan* pLOSS-P_{spac}-*ponA pgcA::tet*	SSB122 → AG211 cells
AG304	*trpC2 amyE::(*$P_{hyspank}$*-mprF, spc)*	pDR111-$P_{hyspank}$-*mprF* → 168CA cells
AG311	*trpC2 ΔponA amyE::(*$P_{hyspank}$*-mprF, spc)*	AG304 → RE101 cells
AG317	*trpC2 ΔponA ΔpbpD ΔpbpF ΔpbpG::kan amyE::(*$P_{hyspank}$*-mprF, spc)*	AG304 → AG157 cells
AG322	*trpC2 amyE::(*$P_{hyspank}$*-mprF, spc) Δmbl::cat*	4261CA → AG304 cells
AG327	*trpC2 amyE::(*$P_{hyspank}$*-mprF, spc) Ωneo ΔmreB*	3725CA → AG304 cells
AG341	*trpC2 ΔponA ΔpbpD ΔpbpF ΔpbpG::kan dltAB::cat*	DLT71 (40) → AG157 cells
AG342	*trpC2 ΔponA ΔpbpD ΔpbpF ΔpbpG::kan ΔltaS::cat*	4285CA → AG157 cells
AG343	*trpC2 ΔponA ΔpbpD ΔpbpF ΔpbpG::kan ΔyfnI::erm*	4289CA → AG157 cells
AG344	*trpC2 ΔponA ΔpbpD ΔpbpF ΔpbpG::kan ΔyqgS::erm*	4294CA→ AG157 cells
AG347	*trpC2 ΔmprF::phleo ΔltaS::cat*	4285CA → AG181 cells
AG349	*trpC2 amyE::(*$P_{hyspank}$*-mprF, spc) ΔltaS::cat*	4285CA → AG304 cells
AG353	*trpC2 amyE::(*$P_{hyspank}$*-mprF, spc) ΔyfnI::erm*	4289CA→ AG304 cells
AG370	*trpC2 ΔponA ΔpbpD ΔpbpF ΔpbpG::kan ΔltaS::cat ΔyfnI::erm*	4289CA → AG342 cells
AG372	*trpC2 ΔponA ΔpbpD ΔpbpF ΔpbpG::kan ΔltaS::cat ΔyqgS::erm*	4294CA → AG342 cells
AG377	*trpC2 ΔponA ΔpbpD ΔpbpF ΔpbpG::kan ΔyqgS::erm ΔyfnI::spc*	4287CA → AG344 cells

AG380	*trpC2 ΔponA ΔpbpD ΔpbpF ΔpbpG::kan ΔltaS::cat ΔyqgS::erm ΔyfnI::spc*	4287CA → AG372 cells
AG383	*trpC2 ΔponA ΔltaS::cat*	4285CA → RE101 cells
AG384	*trpC2 ΔponA ΔyfnI::erm*	4289CA → RE101 cells
AG385	*trpC2 ΔponA ΔyqgS::spc*	4292CA → RE101 cells
AG389	*trpC2 ΔponA ΔpbpD ΔpbpF ΔpbpG::kan ΔmprF::phleo ΔltaS::cat ΔyqgS::erm*	AG223 → AG372 cells
AG390	*trpC2 ΔponA ΔpbpD ΔpbpF ΔpbpG::kan ΔmprF::phleo ΔygqS::erm ΔyfnI::spc*	AG223 → AG377 cells
AG393	*trpC2 ΔponA ΔltaS::cat ΔyfnI::erm*	4289CA → AG383 cells
AG394	*trpC2 ΔponA ΔltaS::cat ΔyqgS::spc*	4292CA → AG383 cells
AG395	*trpC2 ΔponA ΔyfnI::spc ΔyqgS::spc*	4292CA→ AG384 cells
AG399	*trpC2 ΔponA ΔpbpD ΔpbpF ΔpbpG::kan ΔmprF::phleo ΔltaS::cat ΔyfnI::erm*	AG223 → AG370 cells
AG400	*trpC2 ΔponA ΔpbpD ΔpbpF ΔpbpG::kan ΔmprF::phleo ΔltaS::cat ΔyqgS::erm ΔyfnI::spc*	AG223 → AG380 cells
AG403	*trpC2 ΔponA ΔltaS::cat ΔyfnI::erm ΔyqgS::spc*	4292CA → AG393 cells
AG417	*trpC2 ΔpbpD ΔpbpF ΔpbpG::kan*	DPVB45CA → AG105 cells
AG421	*trpC2 ΔpbpD ΔpbpF ΔpbpG::kan amyE::($P_{hyspank}$ mprF, spc)*	AG304 → AG417 cells
AG441	*trpC2 ΔponA ΔltaS::cat ΔyfnI::erm ΔugtP::spc*	PG253 → AG393 cells
AG442	*trpC2 ΔponA ΔltaS::cat ΔyfnI::erm gtaB::TnYLB-1(kan)*	AG200BK#42 → 168CA → AG393 cells
AG443	*trpC2 ΔponA ΔpbpD ΔpbpF ΔpbpG::kan ΔugtP::spc*	PG253 → AG157 cells
AG444	*trpC2 ΔponA ΔugtP::spc*	PG253 → RE101 cells
AG474	*trpC2 ΔcwlO::spc*	PDC463 (43) → 168CA cells
AG475	*trpC2 amyE::($P_{hyspank}$-lytE, spc)*	Dominguez-Cuevas, unpublished → 168CA cells
AG484	*trpC2 ΔponA amyE::($P_{hyspank}$-lytE, spc)*	AG475 → RE101 cells
AG501	*trpC2 ΔponA ΔpbpD ΔpbpF ΔpbpG::kan amyE::($P_{hyspank}$-lytE, spc)*	AG475 → AG157 cells
AG502	*trpC2 ΔponA ΔpbpD ΔpbpF ΔpbpG::kan ΔmprF::phleo amyE::($P_{hyspank}$-lytE, spc)*	AG475 → AG223 cells
AG506	*trpC2 ΔponA ΔgtaB::erm*	SM08 → RE101 cells
AG547	*trpC2 ΔlytE::cat*	This study
AG549	*trpC2 ΔlytE::cat* pLOSS-P_{spac}-*lytE*	pLOSS-P_{spac}-*lytE* →AG547 cells
AG551	*trpC2* pLOSS-P_{spac}-*lytE*	pLOSS-P_{spac}-*lytE* → 168CA cells
AG557	*trpC2 ΔponA* pLOSS-P_{spac}-*lytE*	pLOSS-P_{spac}-*lytE* → RE101 cells

AG565	*trpC2* Ω*lytE-his*$_{12}$::(pMUTin-`*lytE, erm*)	pMUTinHis-'*lytE* → 168CA cells
AG569	*trpC2* Ω*ltaS-his*$_{12}$*::(*pMUTIN-`*ltaS, erm)*	pMUTinHis-'*ltaS* → 168CA cells
AG570	*trpC2* Ω*yfnI-his*$_{12}$*::(*pMUTIN-`*yfnI, erm)*	pMUTinHis-'*yfnI* → 168CA cells
AG586	*trpC2* Δ*cwlO::spc* Ω*lytE-his*$_{12}$::(pMUTin-`*lytE, erm*)	pMUTinHis-'*lytE* → AG474 cells
AG587	*trpC2* Δ*ponA* Ω*lytE-his*$_{12}$::(pMUTin-`*lytE, erm*)	AG565 → RE101 cells
AG588	*trpC2* Δ*ponA* Ω*ltaS-his*$_{12}$*::(*pMUTIN-`*ltaS, erm)*	AG569 → RE101 cells
AG589	*trpC2* Δ*ponA* Ω*yfnI-his*$_{12}$*::(*pMUTIN-`*yfnI, erm)*	AG570 → RE101 cells
AG593	*trpC2 ΔyqgS:spc ΔltaS::cat*	4292CA → 4285CA cells
AG594	*trpC2 ΔyfnI::erm ΔltaS::cat*	4289CA → 4285CA cells
AG595	*trpC2 ΔyfnI::erm ΔyqgS::spc*	4292CA → 4289CA cells
AG600	*trpC2 ΔltaS::cat ΔyfnI::erm ΔyqgS::spc*	4285CA → AG595 cells
AG614	*trpC2 ΔponA ΔpbpD ΔpbpF ΔpbpG::kan ΔmprF::phleo* pLOSS-*P*$_{spac}$*-ponA ΔgtaB::erm*	SM08 → AG210 cells
AG632	*trpC2 ΔponA ΔpbpD ΔpbpF ΔpbpG::kan ΔmprF::phleo ΔugtP::spc*	PG253 → AG223 cells
AG636	*trpC2 ΔponA ΔpbpD ΔpbpF ΔpbpG::kan ΔmprF::phleo ΔgtaB::erm*	AG614 plasmid lost on NA $MgS0_4$ 20 mM with erm
AG1460	*trpC2* Δ*pbpD* Δ*pbpF* Δ*pbpG::kan amyE::(P*$_{hyspank}$*-lytE, spc)*	AG475 → AG417 cells
AG1461	*trpC2* Δ*lytE::cat amyE::(P*$_{hyspank}$*-lytE, spc)*	AG475 → AG547 cells
AG1462	*trpC2* Δ*ltaS::cat amyE::(P*$_{hyspank}$*-lytE, spc)*	AG475 → 4285CA cells
AG1463	*trpC2* Δ*yfnI::erm amyE::(P*$_{hyspank}$*-lytE, spc)*	AG475 → 4289CA cells
AG1465	*trpC2* Δ*ponA* Δ*pbpD* Δ*pbpF* Δ*pbpG::kan* Δ*ltaS::cat amyE::(P*$_{hyspank}$*-lytE, spc)*	AG475 → AG342 cells
AG1466	*trpC2* Δ*ltaS::cat* pLOSS-*P*$_{spac}$*-lytE*	pLOSS-*P*$_{spac}$*-lytE* → 4285CA cells
AG1467	*trpC2* Δ*yfnI::erm* pLOSS-*P*$_{spac}$*-lytE*	pLOSS-*P*$_{spac}$*-lytE* → 4289CA cells
AG1469	*trpC2* Δ*ltaS::cat* Δ*yfnI::erm* pLOSS-*P*$_{spac}$*-lytE*	pLOSS-*P*$_{spac}$*-lytE* → AG594 cells
AG1478	*trpC2* Δ*mprF::phleo amyE::(P*$_{hyspank}$*-lytE, spc)*	AG475 → AG181 cells
AG1479	*trpC2* Δ*ponA* Δ*mprF::phleo amyE::(P*$_{hyspank}$*-lytE, spc)*	AG475 → AG193 cells
AG1480	*trpC2* Δ*ponA* Δ*ltaS::cat amyE::(P*$_{hyspank}$*-lytE, spc)*	AG475 → AG383 cells
AG1481	*trpC2* Δ*mprF::phleo* pLOSS-*P*$_{spac}$*-lytE*	pLOSS-*P*$_{spac}$*-lytE* → AG181 cells

AG1482	*trpC2* Δ*ponA* Δ*mprF::phleo* pLOSS-P_{spac}-*lytE*	pLOSS-P_{spac}-*lytE* → AG193 cells
AG1483	*trpC2* Δ*ponA* Δ*ltaS::cat* pLOSS-P_{spac}-*lytE*	pLOSS-P_{spac}-*lytE* → AG383 cells
AG1486	*trpC2* Δ*mprF::phleo* Ω*lytE-his*$_{12}$::(pMUTin-`*lytE, erm*)	AG565 → AG181 cells
AG1487	*trpC2* Δ*ponA* Δ*mprF::phleo* Ω*lytE-his*$_{12}$::(pMUTin-`*lytE, erm*)	AG565 → AG193 cells
AG1488	*trpC2* Δ*ponA* Δ*ltaS::cat* Ω*lytE-his*$_{12}$::(pMUTin-`*lytE, erm*)	AG565 → AG383 cells
AG1489	*trpC2* Δ*ltaS::cat* Ω*lytE-his*$_{12}$::(pMUTin-`*lytE, erm*)	AG565 → 4285CA cells
AG1490	*trpC2* Δ*ltaS::cat* Δ*yqgS::erm*	4294CA → 4285CA cells
AG1491	*trpC2* Δ*yqgS::cat* Δ*yfnI::erm*	4293CA → 4289CA cells
AG1492	*trpC2* Δ*yqgS::cat amyE::(*$P_{hyspank}$-*lytE, spc)*	AG475 → 4293CA cells
AG1493	*trpC2* Δ*yqgS::cat* pLOSS-P_{spac}-*lytE*	pLOSS-P_{spac}-*lytE* → 4293CA cells
AG1497	*trpC2* Δ*ltaS::cat* Δ*yfnI::erm amyE::(*$P_{hyspank}$-*lytE, spc)*	AG475 → AG594 cells
AG1498	*trpC2* Δ*ltaS::cat* Δ*yqgS::erm amyE::(*$P_{hyspank}$-*lytE, spc)*	AG475 → AG1490 cells
AG1499	*trpC2* Δ*yqgS::cat* Δ*yfnI::erm amyE::(*$P_{hyspank}$-*lytE, spc)*	AG475 → AG1491 cells
AG1500	*trpC2* Δ*ltaS::cat* Δ*yqgS::erm* pLOSS-P_{spac}-*lytE*	pLOSS-P_{spac}-*lytE* → AG1490 cells
AG1502	*trpC2* Δ*yqgS::cat* Δ*yfnI::erm* pLOSS-P_{spac}-*lytE*	pLOSS-P_{spac}-*lytE* → AG1491 cells
AG1535	*trpC2* Δ*ugtP::spc* Ω*lytE-his*$_{12}$::(pMUTin-`*lytE, erm*)	AG565 → PG253 cells
AG1541	*trpC2* Δ*cwlO::spc* Ω*lytE-his*$_{12}$::(pMUTin-`*lytE, erm*)	AG565 → AG474 cells
AG1581	*trpC2* Δ*mbl::zeo amyE::(*$P_{hyspank}$-*mprF, spc)*	AK045B → AG304 cells
AG1593	*trpC2* Δ*mreBH::kan*	BGSC strain* → 168CA cells
AG1594	*trpC2* Δ*ugtP::kan*	BGSC strain* → 168CA cells
AG1604	*trpC2* Δ*ponA* Ω*neo* Δ*mreB*	KS36 → RE101 cells
AG1605	*trpC2* Δ*ponA* Δ*mbl::zeo*	AK045B → RE101 cells
AG1643	*trpC2* Δ*ugtP::kan amyE::(*$P_{hyspank}$-*lytE, spc)*	AG1594 → AG475 cells
AG1663	*trpC2* Δ*mprF::kan*	BGSC strain* → 168CA cells
AG1667	*trpC2* Δ*ltaS::cat* Δ*yfnI::erm amyE::(*$P_{hyspank}$-*lytE, spc)* Δ*mprF::kan*	AG1663 → AG1497 cells

AG1668	*trpC2* Δ*ltaS::cat* Δ*yqgS::erm amyE::(*$P_{hyspank}$*-lytE, spc) ΔmprF::kan*	AG1663 → AG1498 cells
AG1669	*trpC2* Δ*yqgS::cat* Δ*yfnI::erm amyE::(*$P_{hyspank}$*-lytE, spc) ΔmprF::kan*	AG1663 → AG1499 cells
AG1670	*trpC2* Δ*ltaS::cat* Δ*yfnI::erm amyE::(*$P_{hyspank}$*-lytE, spc) ΔugtP::kan*	AG1594 → AG1497 cells
AG1671	*trpC2* Δ*ltaS::cat* Δ*yqgS::erm amyE::(*$P_{hyspank}$*-lytE, spc) ΔugtP::kan*	AG1594 → AG1498 cells
AG1672	*trpC2* Δ*yqgS::cat* Δ*yfnI::erm amyE::(*$P_{hyspank}$*-lytE, spc) ΔugtP::kan*	AG1594 → AG1499 cells
AG1673	*trpC2* Δ*ltaS::cat* Δ*yqgS::spc* Δ*mprF::kan*	AG1663 → AG593 cells
AG1675	*trpC2* Δ*yfnI::erm* Δ*yqgS::spc* Δ*mprF::kan*	AG1663 → AG595 cells
AG1684	*trpC2* Δ*ponA* Ω*lytE-his*$_{12}$::(pMUTin-`*lytE, erm*) *amyE::(*$P_{hyspank}$*-mprF, spc)*	AG304 → AG587 cells
AG1685	*trpC2* Δ*ponA* Ω*lytE-his*$_{12}$::(pMUTin-`*lytE, erm*) Δ*ugtP::kan*	AG1594 → AG587 cells
AK045B	*trpC2 Δmbl::zeo* (in 168CA background)	H. Strahl's lab, A. Koh
Dap^R1	DAP-resistant isolate derived from 168 1A1	(54)
Dap^R20	DAP-resistant isolate derived from 168 1A1	(54)
DLT71CA	*trpC2 dltAB::cat*	DLT71 (40) → 168CA cells
DPVB45CA	*trpC2 ΔpbpG::kan*	DPVB45 (80) → 168CA
HB15507	Dap^R20 $pgsA^{WT}$	(54)
HB15516	Dap^R1 $pgsA^{WT}$	(54)
K532	*trpC2 lacA::cat*	D. Claessen, unpublished
KS36	*trpC2* Ω*neo ΔmreB* (in 168CA background)	H. Strahl's lab, K. Seistrup
PDC620	*trpC2 aprE::(*P_{spac}*-lytE, erm)*	(43)
PDC702	*trpC2 ΔlytE::cat::spc aprE(::*P_{xyl}*-lytE erm)*	(43)
PG253	*trpC2 ΔugtP::spc*	P. Gamba, unpublished
RE101	*trpC2 ΔponA*	(12)
RE102	*trpC2 ΔpbpF*	pG^+host10::*ΔpbpF* (12) → 168CA cells
RE103	*trpC2 ΔpbpD*	pG^+host10::*ΔpbpD* (12) → 168CA cells
RE104	*trpC2 ΔponA ΔpbpD*	pG^+host9::*ΔponA* (12) → RE103 cells
SM08	*trpC2 ΔgtaB::erm*	S. Moore, unpublished
SM31	*trpC2 ggaAB::spc*	S. Moore, unpublished
SM50	*trpC2* Ω*erm* Δ*tagE*	S. Moore, unpublished
SSB122	*trpC2 pgcA (yhxB)::tet*	(81)
SWA11a	*trpC2 ΔponA ΔpbpD ΔpbpF lacA::cat mprF::TnYLB-1(kan)*	This study
S. aureus		

SA113	SA113 (wild type, methicillin-sensitive)	T. Palmer, lab collection
SA113 *ΔmprF*	SA113 *ΔmprF::erm*	(21)

971 [a]Antibiotic resistance to *spc*, spectinomycin; *kan*, kanamycin; *erm*, erythromycin; *neo*,
972 neomycin; *cat*, chloramphenicol; *tet*, tetracyclin; *zeo*, zeocin and *phleo*: phleomycin. *TnYLB-*
973 *1(kan)* transposon that originates from pMarB (**Table 1**). his_{12} indicates a coding sequence that
974 corresponds to a 12 His tag at the C terminus. $P_{hyspank}$ and P_{spac} are IPTG-inducible promoters
975 with $P_{hyspank}$ known to be stronger. Other abbreviations: Δ, deletion; Ω, insertion.
976 [b]Arrows indicate how the strain was constructed by transformation using either a plasmid DNA,
977 a chromosomal DNA (strain code is then indicated) or a PCR on chromosomal DNA. BGSC*
978 refers to the deletion mutant collection of the Bacillus Genetic Stock Center (82).

979 **TABLE 3** Primers used in this study

Primer name	Sequence (in bold restriction enzyme site)	Used for[a]
oAA01	TTTTTCACCTTAATGCTTTGCATGGTATA TCTCCTTCTTAAAGTTAAACAAAATTATT TCTAGAGG	To amplify pET28a (+)
oAA02	ACCTCGGTGCGAAAAGATTCCACCACCA CCACCACCACT	To amplify pET28a (+)
oAA03	TAAGAAGGAGATATACCATGCAAAGCAT TAAGGTGAAAAAAGGCGAC	To amplify *lytE* from base 76th-1002th
oAA04	CAGTGGTGGTGGTGGTGGTGGAATCTTTT CGCACCGAGGTAACG	To amplify *lytE* from base 76th-1002th
oAA05	ACGCCGAAACAAGCGCTC	To check pET28a-*lytE-his* plasmid
oAA06	GCTAGTTATTGCTCAGCG	To check pET28a-*lytE-his* plasmid
oAG18	GTTGACTTTATCTACAAGGT	To check insert cloned in pLOSS-P_{spac}-*lytE*
oAG19	GGTACCAGTAGTTCACCAC	To check pLOSS-P_{spac}-*lytE*
oAG81	GAATCGCCTGGCTCACATCATC	To check *B. subtilis mprF::*TnYLB-1
oAG82	CGGCAAAGAACAGTCCCAAG	To check *B. subtilis mprF::*TnYLB-1
oAG103	CCTGTATGTCTGGCACTCAC	To amplify upstream *mprF*
oAG104	GC**TCTAGA**TGGTCTCTCCAATCATATTC	To amplify upstream *mprF* (*Eco*RI)
oAG105	CG**GAATTC**TAAGACGGAGTCTTTTTTTAT TTCG	To amplify downstream *mprF* (*Xba*I)
oAG106	CGGAGATGCGAGAGGGTTTC	To amplify downstream *mprF*
oAG107	TGCGGCATGCTCATATCCAG	To check *B. subtilis ΔmprF*
oAG108	TGGGCCAATCAGTGGACAAG	To check *B. subtilis ΔmprF*
oAG124	CCATCATCTGGTGCGAAAGG	(12), to check *B. subtilis ΔponA*
oAG125	CCGCAAAGCCGATTAATTGG	
oAG126	TCTATTGGCGAGTGCTTC	(12), to check *B. subtilis ΔpbpF*
oAG127	AGCATCGACTCCGTATTG	
oAG128	TTATTCGGAATGGCGATGGG	(12),to check *B. subtilis ΔpbpD*
oAG129	CCTTAATGGCTGCAGTTGAC	
oAG165	CTAACCTGGCTGACATTCAC	To check *B. subtilis gtaB::*TnYLB-1
oAG166	TGATCAGGTCTTCGCAGTTG	To check *B. subtilis gtaB::*TnYLB-1
oAG197	GC**TCTAGA**GCACCCATTAGTTCAACAAA CG	To amplify *cat* (*Xba*I)
oAG198	GC**GGATCC**AGTACAGTCGGCATTATCTC	To amplify *cat* (*Bam*HI)
oAG271	GGG**GTCGAC**AAAGGAGATTCCTAGGAT GCTGATTAAAAAGAATGCT	To construct pDR111-$P_{hyspank}$-*mprF*
oAG272	GGG**GCATGC**TTGATGATATTGAAACCT	To construct pDR111-$P_{hyspank}$-*mprF*

oAG300	CAATCACGAAACAATAATTGG	To check cloned insert in pDR111
oAG301	GTTGACTTTATCTACAAGGTG	To check cloned insert in pDR111
oAG308	GGG**GCTAGC**AAAGGAGATTCCTAGGATGAAAACATTTATAAAAGAAAGAGG	To construct pDR111-$P_{hyspank}$-*ltaS* (*Nhe*I)
oAG309	CCG**GCATGC**CCGAATGTGGAATTTGC	To construct pDR111-$P_{hyspank}$-*ltaS* (*Sph*I)
oAG310	GGG**GCTAGC**AAAGGAGATTCCTAGGATGAAGAAACTTTTTCTTACAAAC	To construct pDR111-$P_{hyspank}$-*yfnI* (*Nhe*I)
oAG311	CCG**GCATGC**TGTAATGATATGAGAGAAAGC	To construct pDR111-$P_{hyspank}$-*yfnI* (*Sph*I)
oAG312	GGG**GCTAGC**AAAGGAGATTCCTAGGATGCGAAAAACGTTTTTTCGAAG	To construct pDR111-$P_{hyspank}$-*yqgS* (*Nhe*I)
oAG313	CCGGCATGCGAAAGCCTCCCGCTCACTTC	To construct pDR111-$P_{hyspank}$-*yqgS* (*Sph*I)
oAG340	GTCACATGAAGTCAAGACTATT	To check *ΔlytE*
oAG341	ACGGTTTATCAAGGAAGGACTC	To check *ΔlytE*
oAG348	GTG**GCGGCCGC**ATGAAAAAGCAAATCATTACAG	To construct pLOSS-P_{spac}-*lytE* (*Not*I)
oAG349	CCG**GGATCC**GATTGCCCTTTATGAAAATAAG	To construct pLOSS-P_{spac}-*lytE* (*Bam*HI)
oAG350	GTCTGTGCTTGAGGATAAGG	To amplify upstream *lytE* for construction *ΔlytE*
oAG351	GGG**TCTAGA**CTGCTGTCGTAGCTGTAATG	To amplify upstream *lytE* (*Xba*I) for construction *ΔlytE*
oAG352	CCG**GGATCC**GCGAAAAGATTCTAATTTTTAG	To amplify downstream *lytE* (*Bam*HI), for construction *ΔlytE*
oAG353	GATCCGTTTGCGTGTTTC	To amplify downstream *lytE,* for construction *ΔlytE*
oAG354	GGG**GAATTC**GGCGGAACGACAACTTCAG	To construct pMUTin-`*lytE-his*, amplify 3' terminus `*lytE* (no stop codon)
oAG355	GGG**CTCGAG**GAATCTTTTCGCACCGAGG	To construct pMUTin-`*lytE-his*, amplify 3' terminus `*lytE* (no stop codon)
oAG360	GGC**GAATTC**GATTTATTCTCTAAAGACCACG	To construct pMUTin-`*yfnI-his*, amplify 3' terminus `*yfnI* (no stop codon)
oAG361	GGG**CTCGAG**TTTGATTTCTTTCTCCTTGCCG	To construct pMUTin-`*yfnI-his*, amplify 3' terminus `*yfnI* (no stop codon)
oAG366	GGC**GAATTC**CGAAACGGAGACTTTATTTCAC	To construct pMUTin-`*ltaS-his*, amplify 3' terminus `*ltaS* (no stop codon)
oAG367	GGG**CTCGAG**TTTATCTTCGTTATCCTTTGAC	To construct pMUTin-`*ltaS-his*, amplify 3' terminus `*ltaS* (no stop codon)

oAG368	CAAGGTGTGGCATAATGT	To check integration in pMUTinHis
oAG369	GACATCCAGAGGCACTTC	To check integration in pMUTinHis
oAG412	CACCTGGTTTTCTGCTATAGT	To check *B. subtilis ΔgtaB*
oAG413	GTTTAACTCTACAATCAGTG	To check *B. subtilis ΔgtaB*
PhleoXbaI-fw	GC**TCTAGA**TCTTCCTTCAGGTTATGAC	To amplify *phleo* from pIC22 (*Xba*I)
PhleoEcoRI-rev	C**GAATTC**CGCGCCCGATTGCTGAAC	To amplify *phleo* from pIC22 (*Eco*RI)
oAG686	AAGAGAATGCGCCGGAACATC	To amplify *aprE* locus and generate strain AG1676-1677
oAG689	TGACATTCGGCACACTCC	To amplify *aprE* locus and generate strain AG1676-1677

980 [a] *cat,* chloramphenicol resistance*; phleo*, phleomycin cassette; P_{spac} and $P_{hyspank}$ are promoter

981 inducible with IPTG, the latter is known to be stronger; $rep_{pLS20}(GA \rightarrow CC)$, unstable replication

982 in *Bacillus, TnYLB-1* transposon associated to kanamycin resistance.

983 **TABLE 4** Cell morphogenesis changes associated with deletion of LTA-synthase genes
984 combined with class A PBPs null mutants of *B. subtilis*

Strains[a]	**168CA**	***Δ4***	***Δ4 ΔmprF***	***Δ4 ΔltaS***	***Δ4 ΔltaS ΔyfnI***	***Δ4 ΔltaS ΔyqgS***	***Δ4 ΔyfnI ΔyqgS***	***Δ4 ΔltaS ΔyfnI ΔyqgS***[b]
average cell width (µm)	0.8399	0.6595	0.6793	0.6679	0.7269	0.7560	0.6538	0.7666
stdev	0.0469	0.0492	0.0546	0.0550	0.0528	0.0499	0.0513	0.0529
average cell lenght (µm)	3.258	4.557	4.659	4.828	4.873	4.926	4.813	5.312
stdev	0.787	2.075	2.180	2.325	2.240	2.301	1.926	2.651
cells counted	437	419	399	414	426	420	423	416

985 [a]Average of cell width and cell length of strains 168CA, AG157 (*Δ4*), AG342 (*Δ4 ΔltaS*), AG377
986 (*Δ4 ΔyfnI ΔyqgS*), AG370 (*Δ4 ΔltaS ΔyfnI*), AG372 (*Δ4 ΔltaS ΔyqgS*), AG380 (*Δ4 ΔltaS ΔyfnI*
987 *ΔyqgS*) and AG223 (*Δ4 ΔmprF*) analysed in **Fig S3AB**. Standard deviation (stdev) is indicated.
988 [b]Due to the formation of twisted cell chains, the cells measurement of *Δ4 ΔltaS ΔyfnI ΔyqgS*
989 strain was done on the straight regions of the chain.

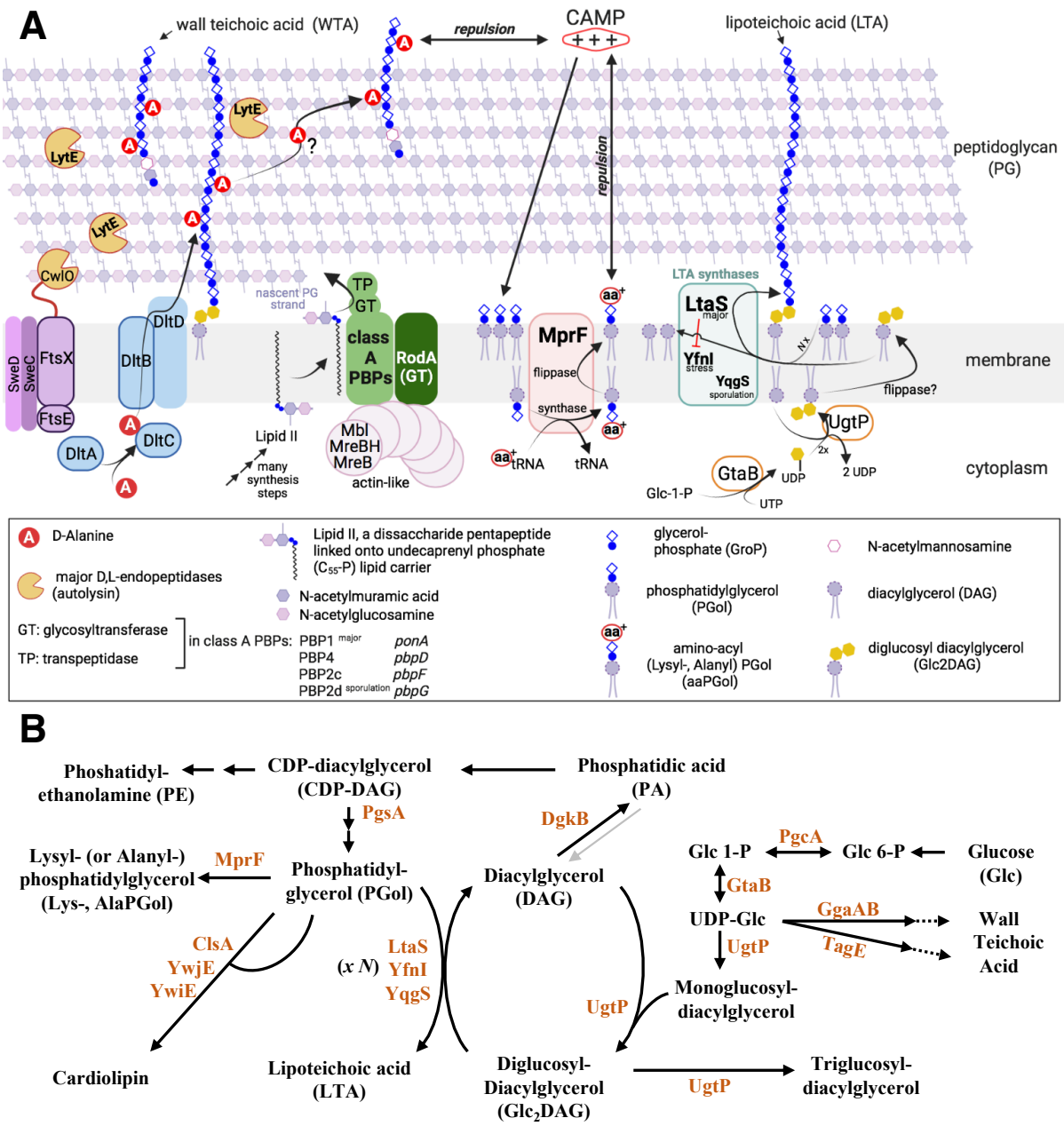

Figure 1. Representations of the cell envelope of Gram-positive rod-shaped bacterium *Bacillus subtilis* and the biosynthetic links between lipoteichoic acids and phospholipids. **(A)** Depiction of some of the cell envelope components and their function in *B. subtilis*. This figure indicates the complexity of the cell envelope synthesis due to the presence of enzymes that seemingly assume the same function. This redundancy of function has been identified in the reaction steps leading to the synthesis of the peptidoglycan (glycosyltransferases: 4 class A PBPs,

996 PBP1/*ponA* major and the essential RodA), the lipoteichoic acids (3 LTA-synthases, where LtaS
997 is the major enzyme) and the actin-like filaments that coordinate the cell shape (3 Mre-
998 homologs: MreB/MreBH and Mbl where the latter is essential in *B. subtilis* 168CA). The major
999 autolysins CwlO and LytE (the absence of both is lethal to *B. subtilis*) cleave the peptidoglycan
1000 pentapeptides. Presence of aminoacyl-phosphatidylglycerol (aaPGols) produced by MprF and the
1001 D-alanylation of teichoic acids by Dlt proteins are thought to create an electrostatic environment
1002 that protects the bacteria from CAMPs (cationic antimicrobial peptides).
1003 **(B)** A schematic representation of the biosynthetic links between lipoteichoic acid,
1004 phospholipids and glucolipids in *B. subtilis*, adapted from previous studies (3, 83). Lipoteichoic
1005 acid (LTA) consist of glycerolphosphate units anchored to the membrane by a glycolipid. In
1006 absence of cytoplasmic UgtP, LTA polymer is linked to the membrane by a diacylglycerol
1007 (DAG), instead of a diglucosyldiacylglycerol (Glc_2DAG). When grown in LB at 37°C, the
1008 majority of *B. subtilis* phospholipids are phosphatidylglycerol (PGol) (37.5% ± 6.2),
1009 phosphatidylethanolamine PE (30.5% ± 3.8), Glc_2DAG (9.6% ± 4.7) and lysyl-
1010 phosphatidylglycerol (LysPGol, 7.8% ± 3.7) produced by MprF (83). Recently, L- and N-
1011 succinyl-LysPGol, and also L- and D-AlaPGol were identified in *B. subtilis* (25). Grey arrow
1012 indicates a reaction step that might be bidirectional.

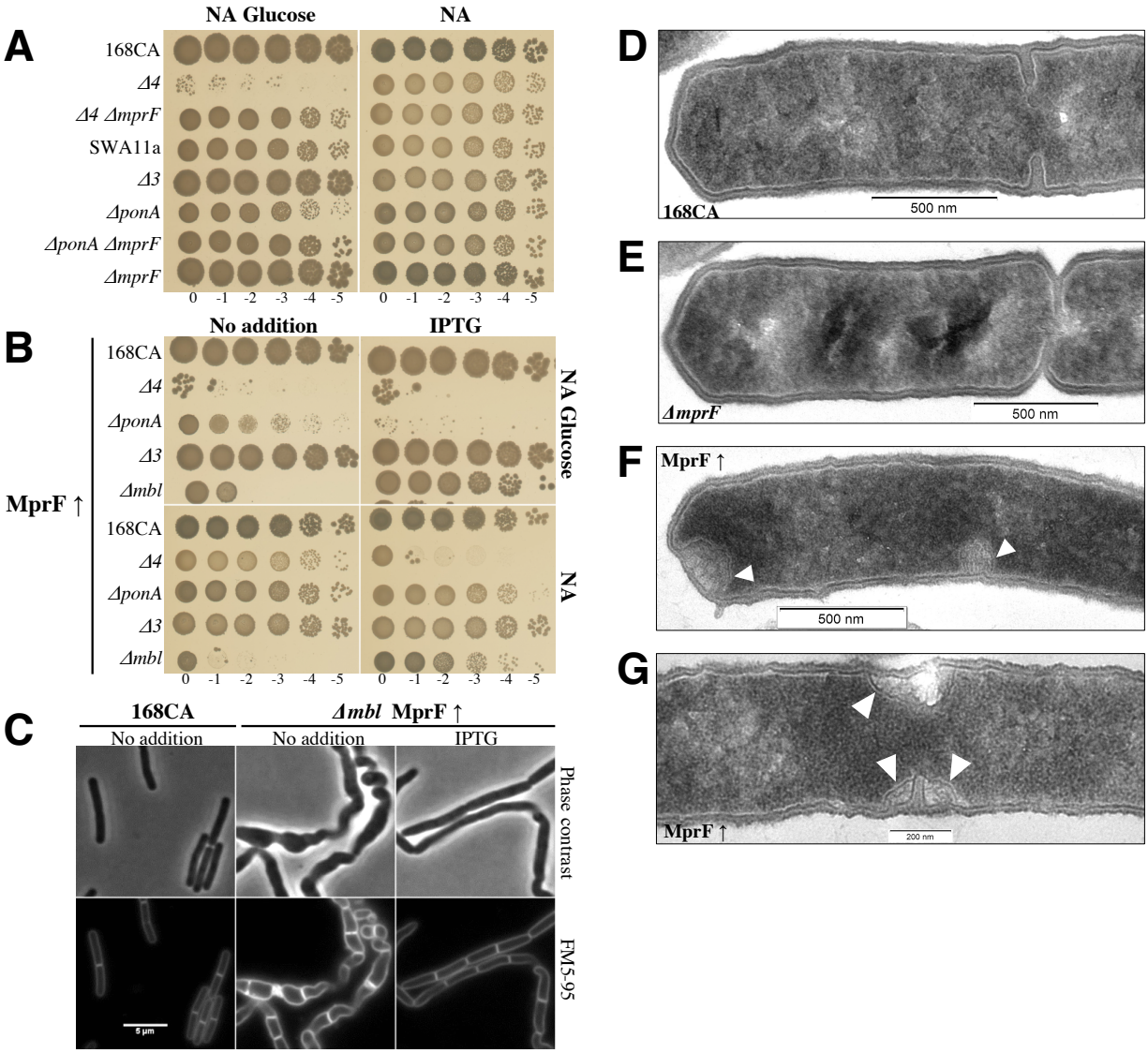

1013 **Figure 2. MprF alters cell viability of *B. subtilis* class A PBPs and *mbl* mutants.**

1014 **(A)** Ten-fold spot growth assays of strains *B. subtilis* wild type 168CA, AG157 (*ΔponA ΔpbpD*
1015 *ΔpbpF ΔpbpG* renamed *Δ4*), AG223 (*Δ4 ΔmprF*), SWA11a (*ΔponA ΔpbpD ΔpbpF*
1016 *mprF::TnYLB-1 lacA*), AG417 (*ΔpbpD ΔpbpF ΔpbpG* renamed *Δ3*), RE101 (*ΔponA*), AG193
1017 (*ΔponA ΔmprF)* and AG181 (*ΔmprF*). Plates (here glucose 1%) were incubated at 37°C for 24 h
1018 and images taken.

1019 **(B)** The effect of *mprF* overexpression (MprF ↑) is assay in different strain backgrounds using
1020 an IPTG-inducible *mprF* construct. Plates (here glucose 1%) were incubated at 37°C for 24 h and

1021 scanned. Strains tested were AG304 (168CA MprF ↑), AG317 (*Δ4* MprF ↑), AG311 (*ΔponA*

1022 MprF ↑), AG421 (*Δ3* MprF ↑) and AG322 (*Δmbl* MprF ↑).

1023 **(C)** Phase-contrast and membrane dye (FM5-95) microscopy images of *B. subtilis* 168CA and

1024 AG322 (*Δmbl* MprF ↑) strains grown in NB ± IPTG (0.1 mM) to mid-exponential phase at 37°C.

1025 Scale bar indicates 5 µm.

1026 **(D-G)** Transmission electron microscopy (TEM) images show cross-sections of (**D**) wild type

1027 168CA, (**E**) AG181 (*ΔmprF)* and (**F-G**) AG304 strain (MprF ↑) grown in nutrient broth (and

1028 IPTG for AG304). Arrows indicate abnormal cell wall structures that seem specific to the strain

1029 MprF ↑. All images were taken at 15,000x magnification and processed in Fiji with scale bars

1030 attached.

1031 Data information. Strains phenotype was tested at least three times, TEM experiment was carried

1032 out one time. Supporting information for this figure is presented in **Fig S1, S2AB**.

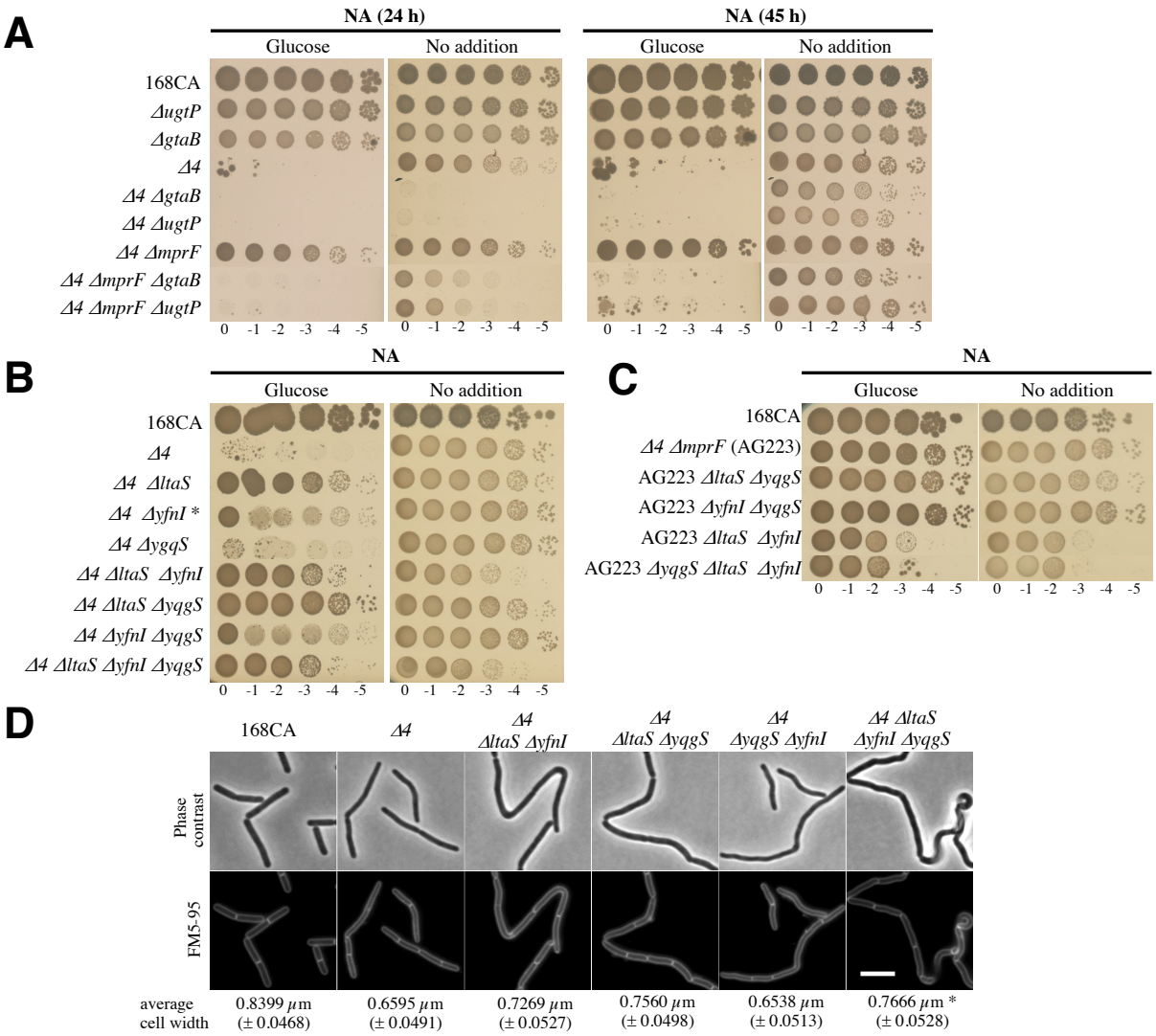

Figure 3. LtaS causes cell morphogenesis defect of an all-class A PBP mutant.

(A) Absence of *gtaB* or *ugtP* causes severe growth defect in absence of class A PBPs and MprF. Strains were grown exponentially in NB with 20 mM $MgS0_4$, then were washed and diluted in NB prior to preparing a 10-fold serial dilution in NB spotting on the NA and NA glucose (0.5%) plates which were incubated at 37°C and imaged after 24 h and 45 h. Strains were also spotted on same media supplemented with 10 mM $MgS0_4$ to confirm all the strains dilution spots could grow, at 17 h of incubation only *Δ4 ΔgtaB* and *Δ4 ΔugtP* displayed colonies of smaller size at that time point (data not shown). Strains tested: *B. subtilis* wild type (168CA), PG253 (*ΔugtP*),

1041 SM08 (*ΔgtaB*), AG157 (*Δ4*), AG290NopLOSS (*Δ4 ΔgtaB*), AG443 (*Δ4 ΔugtP*), AG223

1042 (*Δ4 ΔmprF*), AG636 (*Δ4 ΔmprF ΔgtaB*) and AG632 (*Δ4 ΔmprF ΔugtP*).

1043 **(B)** Spot dilution growth assays for the following strains: *B. subtilis* wild type 168CA, AG157

1044 (*Δ4*), AG342 (*Δ4 ΔltaS*), AG343* (*Δ4 ΔyfnI*), AG344 (*Δ4 ΔyqgS*), AG370 (*Δ4 ΔltaS ΔyfnI*),

1045 AG372 (*Δ4 ΔltaS ΔyqgS*), AG377 (*Δ4 ΔyfnI ΔyqgS*) and AG380 (*Δ4 ΔltaS ΔyfnI ΔyqgS*).

1046 Samples were inoculated onto NA ± glucose 1% and, incubated at 37°C for 24 h. * This strain

1047 was found to pick up suppressor mutations more rapidly than AG342.

1048 **(C)** Ten-fold serial dilutions were prepared for *B. subtilis* wild type 168CA, AG223 (*Δ4 ΔmprF*),

1049 AG389 (AG223 *ΔltaS ΔyqgS*), AG390 (AG223 *ΔyfnI ΔyqgS*), AG399 (AG223 *ΔltaS ΔyfnI*) and

1050 AG400 (AG223 *ΔyqgS ΔltaS ΔyfnI*) strains. Plates (here glucose 1%) were incubated at 37°C and

1051 imaged after 24h.

1052 **(D)** Representative microscopy images of cells of strains of (A) grown in NB at 37°C for 120

1053 min and stained with a FM5-95 dye. Scale bar represents 5 µm. The average of cells diameter

1054 extracted from **Table 4** is indicated. * The cells measurement was done on the straight regions of

1055 the cell chain.

1056 Data information: Strains phenotype was tested at least three times. Supporting information is

1057 presented in **Fig S2C, S3** which also display results obtained in *ΔponA* background.

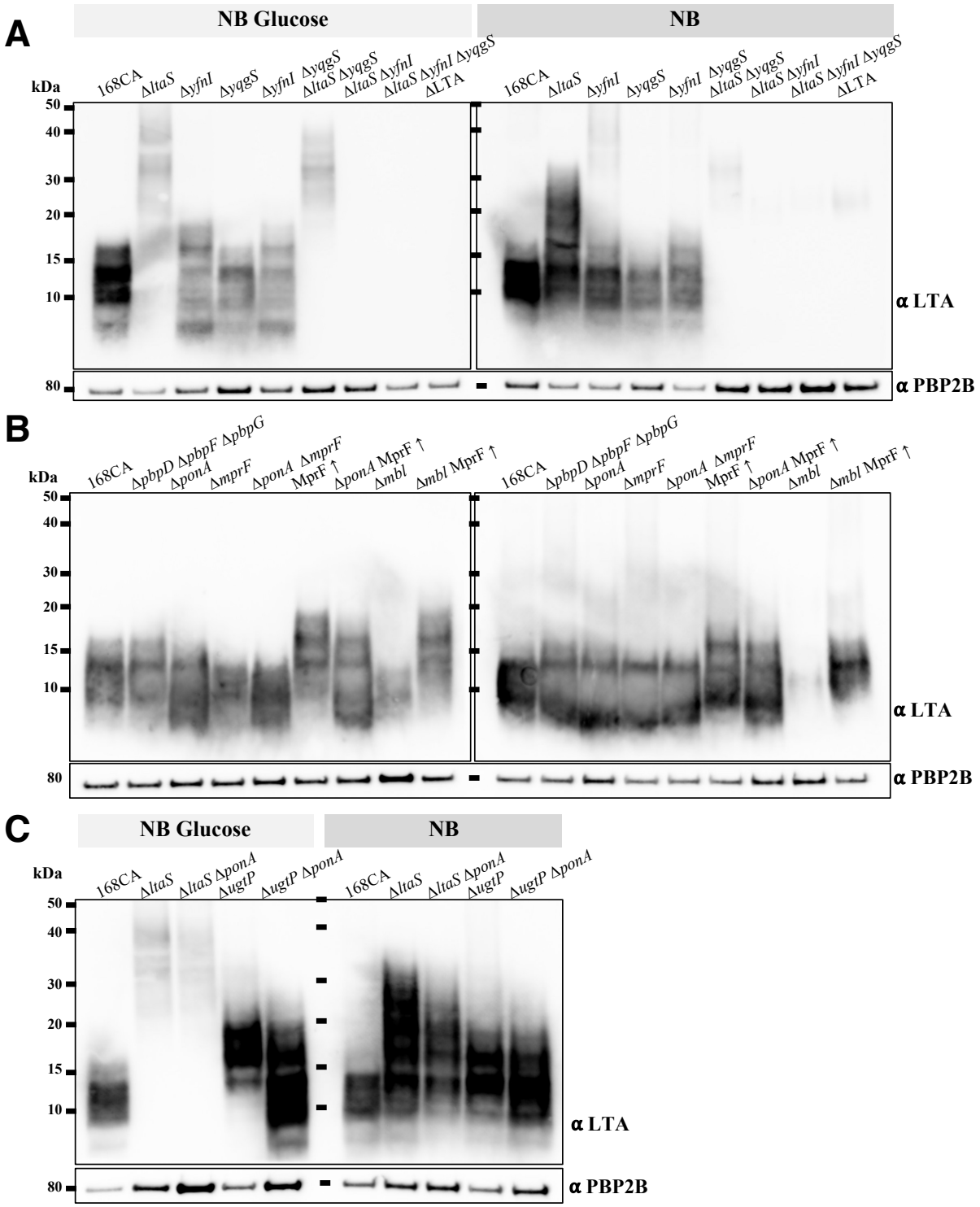

1058 **Figure 4. Analysis of lipoteichoic acid production in *B. subtilis* strains.**

1059 For each set of cultures (NB ± Glucose 0.2%), samples were separated on the same Bis-Tris

1060 gradient gel. Membrane was split at ~ 60 kDa position. The lower part of the membrane was

1061 probed using a monoclonal antibody for Gram-positive LTA and an HRP-linked anti-mouse
1062 antibody. The other membrane part was probed using polyclonal anti-PBP2B and HRP-linked
1063 anti-rabbit antibodies, to provide a sample loading control.
1064 **(A)** Samples were prepared from strains *B. subtilis* wild type (168CA), 4285CA (*ΔltaS*),
1065 4289CA (*ΔyfnI*), 4292CA (*ΔyqgS*), AG595 (*ΔyfnI ΔyqgS*), AG593 (*ΔltaS ΔyqgS*), AG594 (*ΔltaS*
1066 *ΔyfnI*), AG600 (*ΔltaS ΔyfnI ΔyqgS*) and 4620 (*ΔltaS ΔyfnI ΔyqgS ΔyvgJ*, noted here ΔLTA).
1067 **(B)** Strains analysed: *B. subtilis* 168CA, AG417 (*ΔpbpD ΔpbpF ΔpbpG*), RE101 (*ΔponA*),
1068 AG181 (*ΔmprF*), AG193 (*ΔponA ΔmprF*), AG304 (MprF ↑), AG311 (*ΔponA* MprF ↑), 4261CA
1069 *(Δmbl),* AG322 *(Δmbl* MprF ↑). A densitometry graph of the left blot is presented in **Fig S5D**.
1070 **(C)** Samples were extracted from *B. subtilis* 168CA, 4285CA (*ΔltaS*), AG383 (*ΔltaS ΔponA*),
1071 PG253 (*ΔugtP*) and AG444 (*ΔugtP ΔponA*) strains.
1072 Data information: Representative of one of three independent experiments shown in **Fig S4-S6.**
1073 At each section A, B, C, samples were derived from the same experiment.

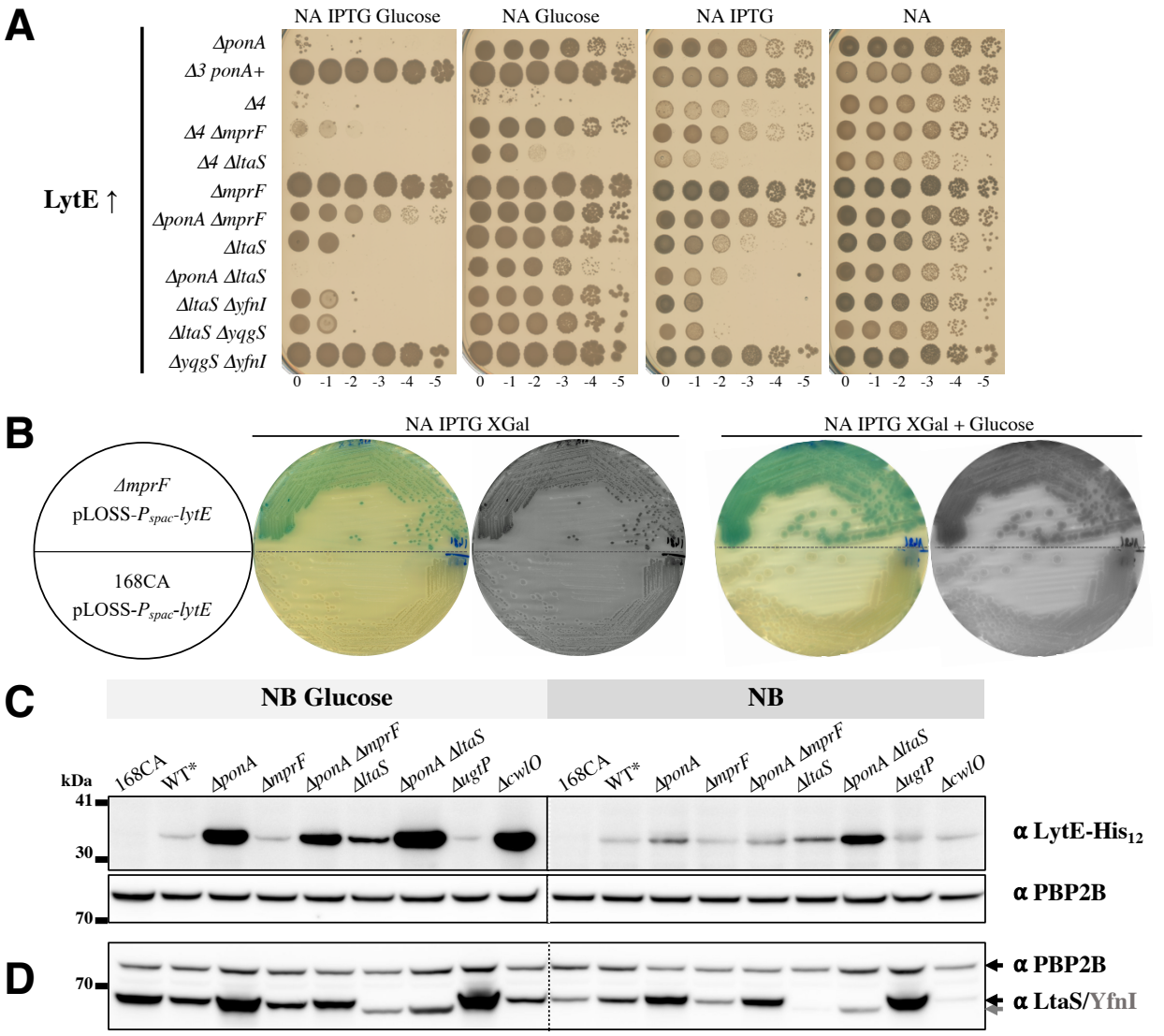

1074 **Figure 5. LytE overexpression is conditionally lethal in absence of PBP1 or LtaS.**

1075 **(A)** *lytE* overexpression was analysed in strains which integrated at the *amyE* locus an (0.1 mM)

1076 IPTG-inducible $P_{hyspank}$-*lytE,* represented here LytE ↑. The strains tested had the following

1077 relevant features: AG484 (*ΔponA* LytE ↑), AG1460 (*Δ3 ponA*$^{+}$ LytE ↑), AG501 (*Δ4* LytE ↑),

1078 AG502 (*Δ4 ΔmprF* LytE ↑), AG1465 (*Δ4 ΔltaS* LytE ↑), AG1478 (*ΔmprF* LytE ↑), AG1479

1079 (*ΔponA ΔmprF* LytE ↑), AG1462 (*ΔltaS* LytE ↑), AG1480 (*ΔponA ΔltaS* LytE ↑), AG1497

1080 (*ΔltaS ΔyfnI* LytE ↑), AG1498 (*ΔltaS ΔyqgS* LytE ↑) and AG1499 (*ΔyqgS ΔyfnI* LytE ↑). The

1081 following strains that did not display any obvious phenotype are not represented here: AG475
1082 (168CA LytE ↑), AG1461 (*ΔlytE* LytE ↑), AG1463 (*ΔyfnI* LytE ↑), AG1492 (*ΔyqgS* LytE ↑).
1083 Plates (here glucose 0.5%) were incubated at 37°C and scanned after 24 h (this figure) and 48 h
1084 (**Fig S7A**).
1085 **(B)** Strains AG1481 (*ΔmprF* pLOSS-P_{spac}-*lytE*) and AG551 (168CA pLOSS-P_{spac}-*lytE*) were
1086 streaked on NA and NA glucose (0.5%), supplemented with IPTG (1 mM) and X-Gal from a
1087 fresh colony on NA spectinomycin. Plates were incubated at 37°C and scanned after 24 h. Blue
1088 colonies indicate the stabilisation of plasmid pLOSS-P_{spac}-*lytE* in *ΔmprF*. Grey scale images are
1089 here to help visualize white colonies.
1090 **(C)** Detection of LytE-His_{12} and PBP2B by Western blots. For simplification on this figure only
1091 the relevant background feature is displayed for the following strains (expressing LytE-His_{12}
1092 under the control of its native promoter): wild-type-like AG565 (WT*), AG587 (*ΔponA*),
1093 AG1486 (*ΔmprF*), AG1487 (*ΔponA ΔmprF*), AG1489 (Δ*ltaS*), AG1488 (*ΔponA ΔltaS*), AG1535
1094 (*ΔugtP*) and AG1541 (*ΔcwlO*). In addition, *B. subtilis* 168CA was grown in parallel (without
1095 antibiotic) and used here as a negative control for the LytE-blot. The membrane was split and
1096 incubated either with a monoclonal Penta-His and an HRP-linked anti-mouse antibodies or with
1097 a polyclonal anti-PBP2B and HRP-linked anti-rabbit antibodies. Note: a 'ladder' sample loaded
1098 after the NB-Glucose (0.2%) sample set is not displayed and the image editing is symbolised by
1099 the vertical black line (see original on **Fig S7B,** middle panel).
1100 **(D)** Detection of LTA-synthases LtaS/YfnI and PBP2B by Western blots. The samples used in
1101 experiment **C** were loaded on a new SDS-gel and the Western blot was carry out with polyclonal
1102 anti-LtaS (able to detect YfnI, unpublished Errington's lab), anti-PBP2B antibodies, and HRP-
1103 linked anti-rabbit antibodies.

1104 Data information: One representative set of three independent Western Blot experiments is

1105 shown here and in **Fig S7B, S8A**. Additional supporting information is presented in **Fig S8, S9**.

1106 At each section samples were derived from the same experiment.

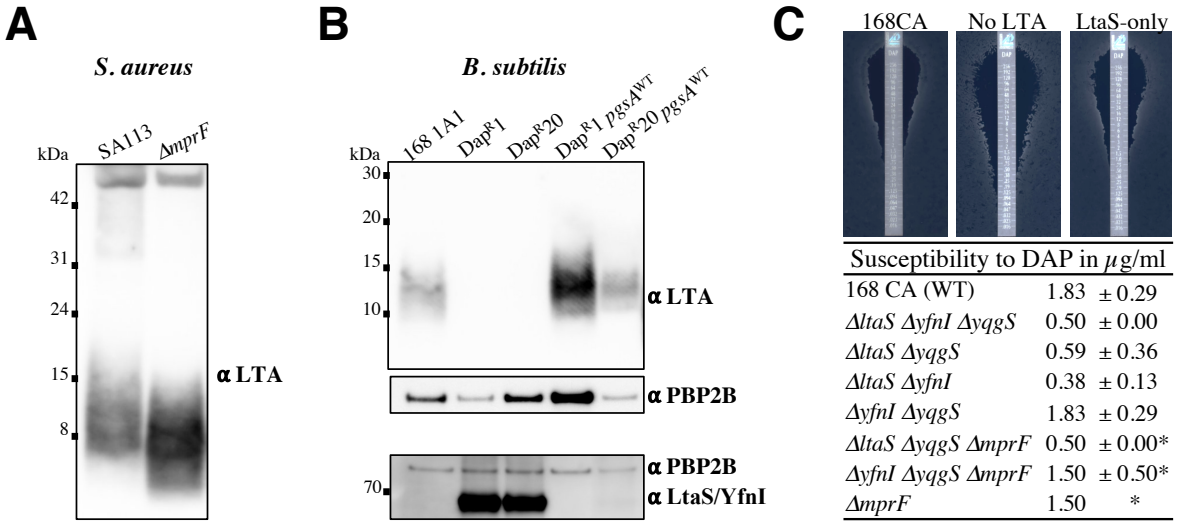

Susceptibility to DAP in μg/ml		
168 CA (WT)	1.83	± 0.29
ΔltaS ΔyfnI ΔyqgS	0.50	± 0.00
ΔltaS ΔyqgS	0.59	± 0.36
ΔltaS ΔyfnI	0.38	± 0.13
ΔyfnI ΔyqgS	1.83	± 0.29
ΔltaS ΔyqgS ΔmprF	0.50	± 0.00*
ΔyfnI ΔyqgS ΔmprF	1.50	± 0.50*
ΔmprF	1.50	*

Figure 6. Daptomycin resistance and LTA synthesis in *B. subtilis* and *S. aureus*.

(A) Samples of methicillin-sensitive *Staphylococcus aureus* strains SA113 and SA113 *ΔmprF* (21) were probed for LTA by Western Blot.

(B) Researchers identified that a modified allele of *pgsA*(*A64V*) was the major determinant of daptomycin resistance of *B. subtilis* Dap^{R}1 and Dap^{R}20 strains selected by serial daptomycin antibiotic passages (54). The strains 168 1A1 (wild type, WT), Dap^{R}1, Dap^{R}20, HB15516 (Dap^{R}1 *pgsA*^{WT}) and HB15507 (Dap^{R}20 *pgsA*^{WT}) were grown in NB overnight at 30°C and LTA was detected (top panel) along with PBP2B (middle panel) by Western Blots. Analysis of the samples grown exponentially at 37°C using theses overnight cultures is presented in **Fig S10F**. The bottom panel shows the cellular abundance of the LTA-synthase detected with an anti-LtaS (that also cross reacts with YfnI, unpublished Errington's lab). Here the samples were normalized based on the previous PBP2B blot (middle panel) (blotted as in **Fig 5D**).

Data information: One representative set of three experiments is shown here and in **Fig S10F**.

(C) Absence of LTA-synthase LtaS increase *B. subtilis* susceptibility to daptomycin. Dap strip assays (Liofilchem) on NA-$CaCl_2$ plates were carried out on *B. subtilis* wild type (168CA),

1122 AG600 (*ΔltaS ΔyfnI ΔyqgS,* noted no LTA), AG593 (*ΔltaS ΔyqgS*), AG594 (*ΔltaS ΔyfnI*), AG595

1123 (*ΔyfnI ΔyqgS,* noted LtaS-only), AG1673 (*ΔltaS ΔyqgS ΔmprF*), AG1675 (*ΔyfnI ΔyqgS ΔmprF*)

1124 and AG1663 (*ΔmprF*) strains. Plates were incubated at 37°C and scanned after 24h (illustrations

1125 on top panel). * The table represents the average of at least two independent experiments except

1126 for *ΔmprF*.

1127 Data information: Additional supporting information is presented in **Fig S10**

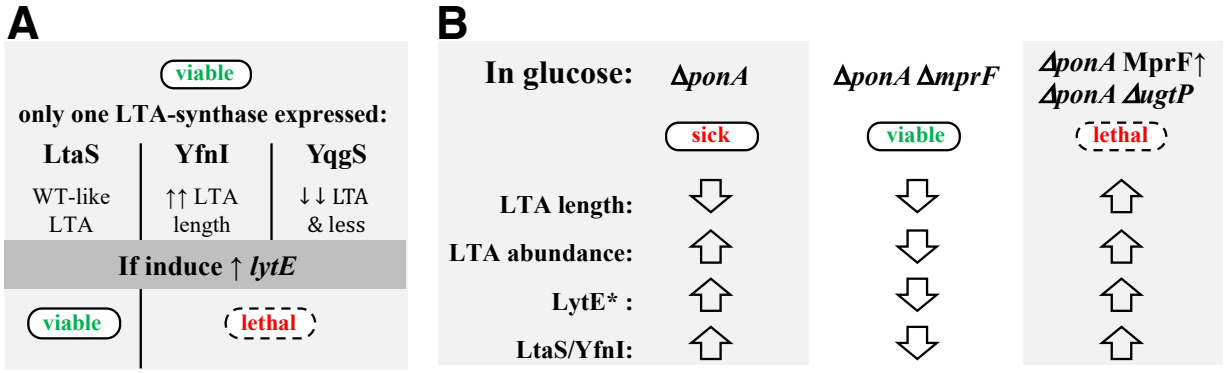

Figure 7. A summary of the alteration in LTA and LytE levels associated with the conditional lethality of *ΔltaS* and *ΔponA* mutants.

(A) The overexpression of *lytE* (inducible) in the double LTA-synthase mutants is lethal except when the major LTA synthase LtaS is functional. The presence of a distinct LTA length is presented by the mutant strains (**Fig 4A, 5A**).

(B) In glucose, the viability and lethality of mutants in *ΔponA* background were associated to distinct LTA, LytE and LtaS/YfnI levels (**Fig 2A-B, 3A, 4B-C, 5A, C-D**). * The overexpression of *lytE* (inducible) is lethal to *ΔponA* but not to *ΔponA ΔmprF* mutant (**Fig 5A**).

Strains with the ability to grow without significant cell lysis are referred as viable (green text in the cell). Lethal refers to an absence of growth of the mutant on NA or in the specified condition (dashed rod cell, with red text). In these cases, analysis of the strains was done by shifting cultures to non-permissive conditions (e.g. low magnesium, addition of glucose or inducer). Arrows indicate an increase (↑) or decrease (↓) of the specified factor. Here it is assumed that the strength of LTA signal observed by Western blot is proportional to abundance.

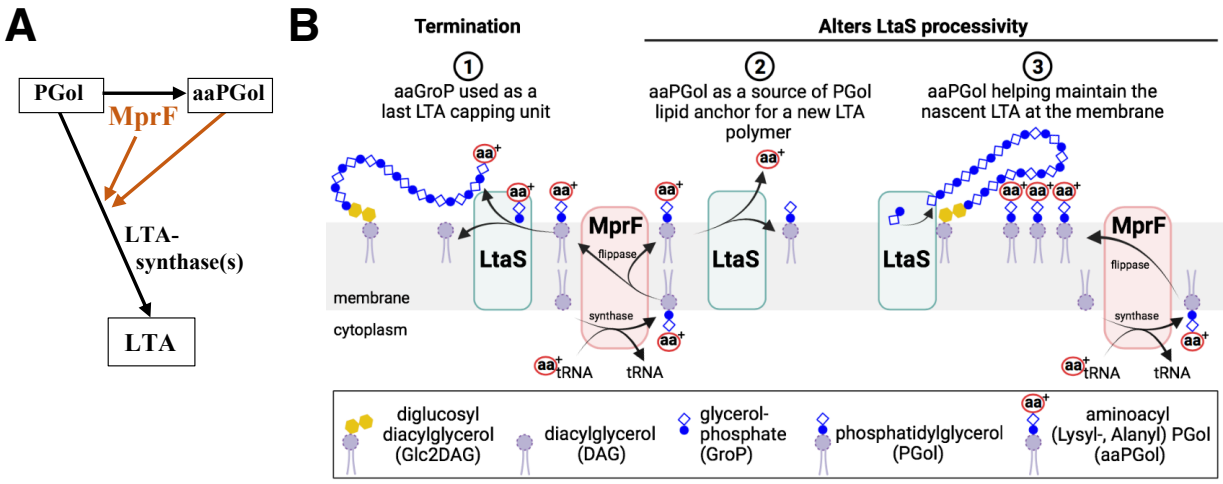

Figure 8. MprF positively regulates the synthesis of LTA in *B. subtilis* and *S. aureus*

(**A**) MprF or its substrates positively regulate LTA production in *B. subtilis* and in *S. aureus.* (**B**) Proposed role of MprF in LTA production via its substrate aminoacyl-phosphatidylglycerols (aaPGol) (not limitative). (**1**) LtaS could use the aminoacyl-glycerol-phosphate (aaGroP) of aaPGol as a last LTA capping unit. Potentially the addition of this positive charged capping unit (e.g. lysyl, alanylGroP) could contribute to the protection against CAMPs. (**2-3**) MprF could indirectly alters LtaS processivity: the release of the aminoacyl could permit LtaS to use the PGol as lipid anchor (**2**), the presence of aaPGol in the vicinity of LtaS could create an electrostatic environment that help maintain the growing LTA chain in a conformation that favors LtaS processing (**3**).